UiT
THE ARCTIC
UNIVERSITY
OF NORWAY

Faculty of Science and Technology

# Thermography and tensile tests of steel samples

*Study of material properties and internal friction effects*

**Even Stange**

*Master thesis in Technology and Safety in the High North, June 2018*

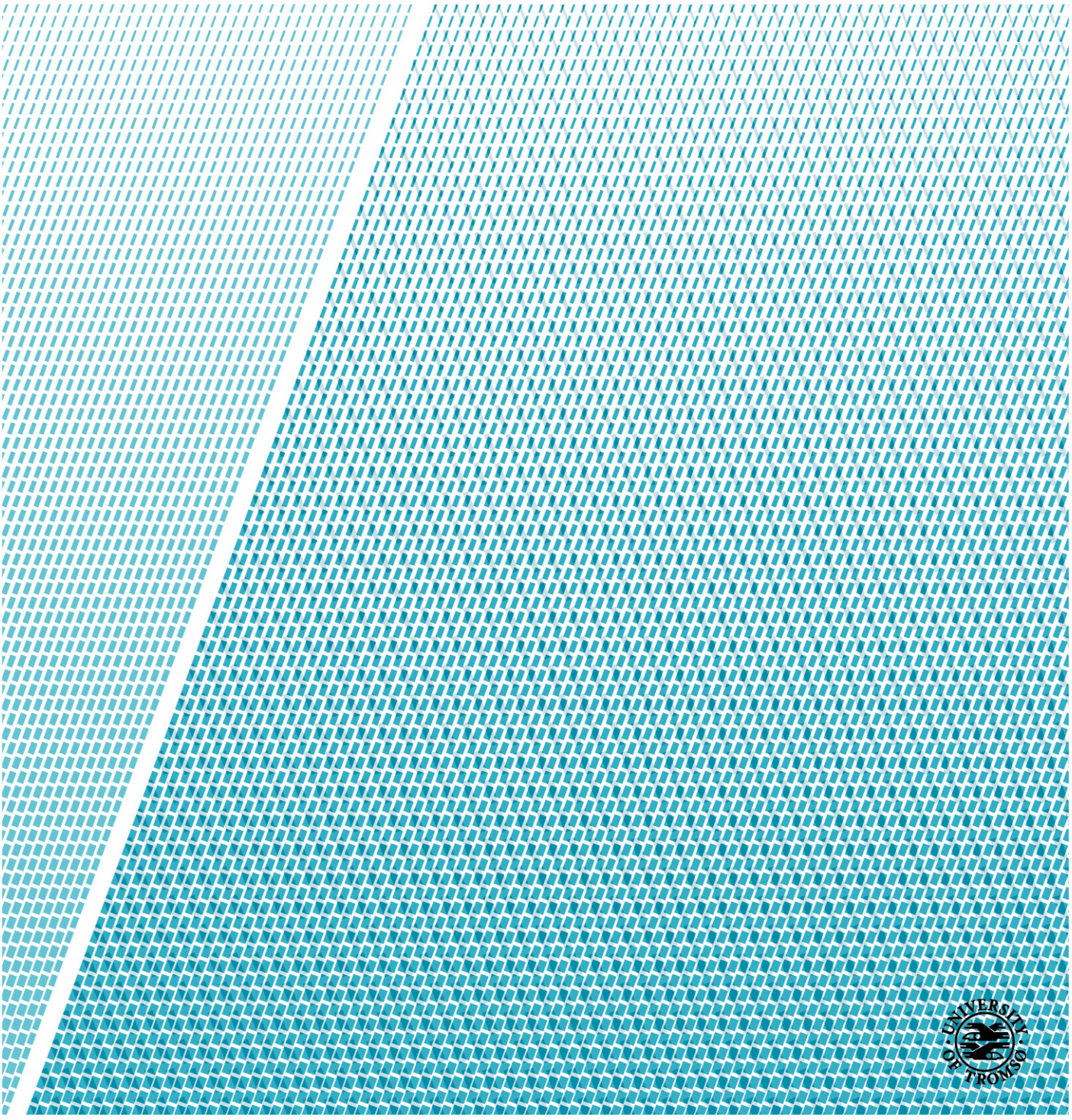

# Project Report – Page 2

**UiT, The Arctic University of Norway**

**Faculty of Science and Technology**

| | |
|---|---|
| Field of study: Master Thesis TEK-3901 | Year: 2018 |
| Title:<br>Thermography and tensile tests of steel samples | Date:<br>$1^{st}$ of June<br><br>Grading:<br>Unclassified<br><br>Number of pages:<br>45 |
| Author:<br>Even Stange | |
| Confidentiality:<br>Open | |
| Supervisor:<br>Hassan Abbas Khawaja | |
| Contracting authority and assigner:<br>UiT, The Arctic University of Norway | |

Abstract:
The thesis presents analysis of material properties and internal effects in steel samples, with varying temperatures. Uniaxial tensile tests were conducted in both room temperature and low temperatures, to generate graphical measures of the mechanical properties. The steel samples were monitored with thermography throughout the course of the tensile tests, to investigate the heat generation associated with internal effects. The analysis is limited to observations of change with temperature, and do not discuss the desirability. A numerical analysis with the finite element method was conducted for qualitatively comparison with the physical experiments.

Keywords:
Experimental tensile tests, Thermography, Steel Properties, Internal Friction, Thermoelastic Effects, Heat Generation, Finite Element Method

## Preface and Acknowledgements

This thesis concludes my master's degree in Technology and Safety in the High North at the University of Tromsø. The work for this thesis was completed at the Faculty of Science and Technology, in the time period from January to June, 2018.

I would like to acknowledge my supervisor, Dr. Hassan Abbas Khawaja, for assistance and guidance throughout the work of this thesis. I would also like to thank the faculty for the financial support, which made it possible to carry out the experiments in this thesis.

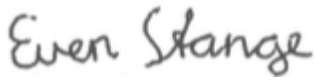

Even Stange

Tromsø, June 2018

## Abstract

The thesis presents analysis of material properties and internal effects in steel samples, with varying temperatures. Uniaxial tensile tests were conducted in both room temperature and low temperatures, to generate graphical measures of the mechanical properties. The steel samples were monitored with thermography throughout the course of the tensile tests, to investigate the heat generation associated with internal effects. The analysis is limited to observations of change with temperature, and do not discuss the desirability. A numerical analysis with the finite element method was conducted for qualitatively comparison with the physical experiments.

# Contents

# List of Figures



# List of Tables

# 1 Introduction

## 1.1 Background

The natural resources in the Arctic regions are attracting the industry. New offshore oil and gas fields are being developed, the maritime transport are growing, and industrialised fisheries move farther north in the Arctic waters. Consequently, new industrial facilities will be developed in the cold and hostile Arctic environment. The industry will face challenges in the design of structures and equipment for low-temperature application. The performance of many structures and components is seriously affected in very cold climates. At low temperatures materials tend to become hard and *brittle*; as a result, concerns are raised about their reliability and safety in such cold climate [1]. The need for cold regions engineers with a solid understanding of the behaviour of materials, is essential for the evaluation and selection of suitable materials. This can ensure that an adequate safety margin is maintained in material performance and requirements.

The development history of practice in many engineering disciplines is, in large part, the story of failures. Several 20th-century calamities have markedly contributed to improving engineering practices [2]. The story of Titanic is a very known tragic tale of life lost, and the most famous of all shipwrecks. The ship was designed with the latest safety features at the time of construction, and was thought to be *unsinkable*. April 12, 1912, on her maiden voyage, the liner RMS Titanic struck an iceberg in the Atlantic and sank, with a loss of over 1500 people. Many questions were raised as to how and why Titanic sank as she did. Metallurgical and mechanical analyses of the hull material recovered from the wreck indicated that the steel possessed a ductile-to-brittle transition temperature that was very high with respect to the service temperature, making the material brittle at ice-water temperatures [3]. If the steel hadn't been so brittle at the operating temperatures, the fate of many of its passengers might have been different.

## 1.2 Problem Description

The decision as to the structure design is governed by the purpose of which the structure is required, the materials that are to be used and any aesthetic considerations that may apply [5]. Analysing stress-strain relations in structural materials are essential in order to measure technological characteristics and to estimate mechanical properties of materials. This are usually determined by laboratory tests, where the strength and limits are found by testing a specimen of a certain form in a certain manner. To apply these results in engineering design requires an understanding of the effects of many different variables, such as internal effects, temperature and method of loading.

Cold regions climatic conditions should not impair the structures reliability and durability. Analysing stress-strain relations and internal effects for material to be used in these conditions are especially important. The loss of ductility in a metal can be observed by examining its low temperature stress-strain relationship. As the temperature is lowered, both the yield point (where ductility begins) and the ultimate strength point (where failure occurs) may shift to a higher stress value, but the fracture may begin at a much lower strain value [1].

## 1.3 Aim and Objective

The primary objective of the thesis is to perform thermograhy and experimental tensile tests of steel samples in varying temperatures. The aim is to observe the change in material properties and internal effects, by analysing the generated stress-strain diagrams and infrared images of the steel samples. The second objective of the thesis is to carrie out a numerical tensile test, with the Finite Element Method.

1. Stress-strain analysis: Study the change in steel properties with varying temperatures
2. Thermography analysis: Study the internal friction effects in steel
3. Numerical analysis: Qualitative comparison with the physical experiments.

## 1.4 Limitations

The following limitations are established for the study of this thesis:

- The analysis are limited to a specific material
- The material is analysed in a limited temperature rage
- The material is tested with a fixed loading rate

## 1.5 Thesis overview

- Chapter (2): This chapter presents the theoretical framework of this study, to establish a foundation for the reader. The chapter includes among other things fundamental principles, analysis methods and thermography.

- Chapter (3): This chapter presents the experimental- and numerical methodology used in the study of this thesis. The test and simulation procedures are explained, with detailed overview of the equipments, softwares and raw-data acquisition.

- Chapter (4): This chapter presents and discuss the results from the analysis. The chapter is divided into subchapters by the different analysis, directly related to the objectives; Stress-strain analysis, thermography analysis, numerical analysis.

- Chapter (5): This chapter presents the summary and conclusion of the author, based on the results from the experimental and numerical analysis.

- Chapter (6): The last chapter presents suggestions for further work of this study.

# 2 Literature review

This chapter is intended to provide the theoretical framework which describes the major topics on which this thesis is founded. Firstly, the reader is introduced to fundamental principles associated with stress analysis. Thereafter, the mechanics of structural materials and analysing methods are discussed. Following is an introduction to thermodynamics and the mechanism of heat transfer. Lastly, the phenomenon of internal friction and the thermoelastic effect are discussed.

## 2.1 Fundamental Principles

### 2.1.1 Stress and Strain

In everyday language, the expression *force* is considered as a push or pull. In the context of basic engineering, force ($F$) is defined as an interaction between two bodies or between a body and its environment. The force can be quantified as *stress*, which characterises the strength of the force, on a force per unit area. The associated quantity, *strain*, describes the resulting deformation caused by the stress. When the stress and strain are small enough, we often find that the two are directly proportional, and we call the proportionality constant an elastic modulus [6]. If we apply a force of equal magnitude but opposite directions at the ends of a body, we say that the object is in tension. The stress are defined as the ratio of the force to the cross-sectional area of the body, and is denoted by the Greek letter sigma $\sigma$:

$$Stress, (\sigma) = \frac{F}{A} \tag{1}$$

The SI unit of stress is the *Pascal* ($Pa$), which equals newton per square meter ($N/m^2$). The following strain is denoted by $\varepsilon$ and is equal to the fractional change in length caused by the stress, which is the ratio of the elongation length to the original length. Since length and elongation have the same units, the strain is a dimensionless quantity [7]. Mathematical, we can express the strain by:

$$Strain, (\varepsilon) = \frac{\Delta L}{L} \tag{2}$$

When a body is either at rest or moving with constant velocity (in a straight line with constant speed), we say that the body is in equilibrium. For a body to be in equilibrium, it must be acted on by no forces, or by several forces such that their vector sum - that is, the net force - is zero [6]. The definition of equilibrium corresponds with newtons first laws of motion - the sum of net forces equals zero.

### 2.1.2 Work and Energy

The everyday meaning of *work* is any activity that requires muscular or mental effort. In engineering, work has a much more precise definition. On the basis of classical mechanics, parts of which are presented in section 2.1.1, the concepts of work, kinetic energy and potential energy was provided. Work can be defined as a means for transferring energy. Accordingly, the term work does not refer to what is being transferred between systems or to what is stored within

systems. Energy is transferred and stored when work is done [6]. The total work done on a particle by external forces is related to the particles displacement - that is, to changes in its position. The *kinetic energy* of the particle equals the amount of work required to accelerate the particle from rest to a certain speed, or of being brought to rest [7]. The SI unit of work (W) is the *joule* ($J$), 1 joule is equivalent to 1 *newton-meter*.

$$W = F \times s, (N \times m) \tag{3}$$

In a given process, the total energy of the system is considered to be made up of three macroscopic contributions - kinetic energy ($KE$), potential energy ($PE$) and *internal energy* ($U$). These contributors may all change, but the sum of changes in the system is always zero. The change in kinetic- and potential energy are associated with the motion of the system as a whole. All other energy changes are lumped together in the internal energy of the system. Part of the internal energy is translational kinetic energy of the molecules. Other contributions include the kinetic energy due to rotation of the molecules relative to their center of mass and the kinetic energy associated with vibrational motions within the molecules [8].

### 2.1.3 Temperature and Heat

The terms *temperature* and *heat* are often used interchangeably in everyday language. Temperature depends on the physical state of a material and express the hotness or coldness quantitatively by temperature scales - *Celsius* ($°C$), *Fahrenheit* ($°F$) and absolute temperature *Kelvin* ($K$). In engineering, the term *heat* always refers to energy in transit from one body or system to another because of a temperature difference, never to the amount of energy contained within a particular system [6]. We can change the temperature of a body by adding heat to it or taking heat away, or by adding or subtracting energy in other ways, such as mechanical work. Energy transfer that takes place solely because of a temperature difference is called heat flow or heat transfer. The symbol Q denotes an amount of energy transferred across the boundary of a system in a heat interaction with the system's surroundings.

Q $> 0$: heat transfer *to* the system
Q $< 0$: heat transfer *from* the system

An *adiabatic process* is defined as one with no heat transfer into or out of a system; $Q = 0$. We can prevent heat flow either by surrounding the system with thermally insulating material or by carrying out the process so quickly that there is not enough time for appreciable heat flow. An *isothermal process* is a constant-temperature process. For a process to be isothermal, any heat flow into or out of the system must occur slowly enough that thermal equilibrium is maintained. Any energy entering the system as work ($W$) must leave it again as heat ($Q$) done by the system. In mechanics, equilibrium means a condition of balance maintained by a equality of opposing forces. In thermodynamics, the concept is far more far-reaching, including not only a balance of forces but also a balance of other influences. Each kind of influence refers to a particular aspect of thermodynamic, or complete, equilibrium. Accordingly, several types of equilibrium must exist individually to fulfil the condition of complete equilibrium; among these are mechanical, thermal, phase, and chemical equilibrium [8].

## 2.2 Mechanics of Materials

This discussion pertains to the behavior of what are commonly designated as structural materials. That is, materials suitable for structures and members that must sustain loads without suffering damage. The mechanical properties of a material are usually determined by laboratory tests, and the commonly accepted values of ultimate strength, elastic limit, etc., are those found by testing a specimen of a certain form in a certain manner. To apply results so obtained in engineering design requires an understanding of the effects of many different variables, such as form and scale, temperature and other conditions of service, and method of loading [9].

### 2.2.1 Methods of Loading

The method of loading, in particular, affects the behaviour of bodies under stress. There are an infinite number of ways in which stress may be applied to a body, but for the purpose of material tests, it is sufficient to distinguish the types of loadings which are listed below [9]. The method selected are dependent on the characteristics and properties desired to obtain. Many material tests, with different methods of loading, may be performed for a selected material to obtain a solid understanding of its behaviour under stress.

1. Short-time static loading: *The load is applied so gradually that at any instant all parts are essentially in equilibrium. In testing, the load is increased progressively until failure occurs, and the total time required to produce failure is not more than a few minutes.The ultimate strength, elastic limit, yield point, yield strength, and modulus of elasticity of a material are usually determined by short-time static testing at room temperature.*

2. Long-time static loading: *The maximum load is applied gradually and maintained. In testing, it is maintained for a sufficient time to enable its probable final effect to be predicted. The creep, or flow characteristics, of a material and its probable permanent strength are determined by long-time static testing at the temperatures prevailing under service conditions.*

3. Repeated loading: *Typically, a load or stress is applied and wholly or partially removed or reversed repeatedly. This type of loading is important if high stresses are repeated for a few cycles or if relatively lower stresses are repeated many times.*

4. Dynamic loading: *The circumstances are such that the rate of change of momentum of the parts must be taken into account. One such condition may be that the parts are given definite accelerations corresponding to a controlled motion, such as the constant acceleration of a part of a rotating member or the repeated accelerations suffered by a portion of a connecting rod. As far as stress effects are concerned, these loadings are treated as virtually static and the inertia forces are treated exactly as though they were ordinary static loads.*

### 2.2.2 Elasticity

*Elasticity* is the property of materials to return to its original shape and size when forces causing a deformation are removed. Elastic deformations are termed reversible; the energy expended in deformation is stored as elastic strain energy and is completely recovered upon load removal. Most solid materials exhibit elastic behaviour, to a greater or lesser extent. The limit of which elastic recovery is possible for any given material, called *the elastic limit*, is the maximum stress that can arise before the onset of permanent deformation. Stresses beyond this limit cause a material to *yield*, marking the end of elastic behaviour and the beginning of *plastic behaviour*. The law of elasticity, generally known as *Hooke's law*, states that the force ($F$) and its resulting deformation ($x$) is related linearly as long as the force is sufficiently small [10].

$$\{F\} = \{k\}\{x\} \tag{4}$$

Where $k$ is a constant of proportionality called the stiffness, which is a measure of the load needed to induce a given deformation in the material, expressed by the units of $(N/m)$. A useful way to adjust the stiffness to be a purely materials property is to normalize the load and deformation by stress and strain, which its relations are described in section 2.1.1. Using these more general measures of load per unit area and displacement per unit length, Hooke's Law becomes [10]:

$$\sigma = E\varepsilon \tag{5}$$

The constant of proportionality E, called Young's modulus or the modulus of elasticity, is one of the most important mechanical descriptors of a material. Expressed by the same units as stress, *Pascal* $(Pa)$. In determining stress by the mathematical analysis, it is customary to assume that material is elastic and that it conforms to Hooke's law. However, very careful experiments show that for all materials there is probably some set and some deviation from Hooke's law for any stress, however small [9].

### 2.2.3 Plasticity

*Plasticity* is the property of materials to flow or change shape permanently when subjected to stresses of intermediate magnitude between the elastic limit and those causing failure of the material, or rupture. Plastic deformation are termed irreversible, in the sense that permanent deformations involve the dissipation of energy. The classical theory of plasticity grew out of the study of metals in the late nineteenth century. It is concerned with materials which initially deform elastically, but which deform plastically upon reaching a yield stress [11]. Elastic deformation represents an actual change in the distance between atoms or molecules; plastic deformation represents a permanent change in their relative positions. In metals and other crystalline materials, this permanent rearrangement consists largely of displacements of the atoms in the crystal lattice [9].

Analysis of metal plasticity can be categorised in two broad groups. The first involves relatively small plastic strains, often of the same order as the elastic strains which occur. The second type of problem involves very large strains and deformations, so large that the elastic strains can be disregarded. Analysis of small plastic strains are used in the design of structures, were plasticity is seen as a material failure. Analysis of large strains are used in the manufacturing and forming processes of metals [11].

### 2.2.4 Ductile and Brittle

Among the various material properties introduced, this discussion pertains to the study of those effects associated with metals. Furthermore, it is convenient to divide metas into two classes: (1) *Ductile* metals, in which marked plastic deformation commences at fairly definite stress (yield point, the elastic limit) and which exhibit cinsiderable ultimate elongation. (2) *Brittle* metals for which the beginning of plastic deformation is not clearly defined and which exhibit little ultimate elongation [9]. As mentioned in section 2.2.3, metals undergoes a rearrangement of its internal molecular structure in plastic deformations, which requires a mechanism for molecular mobility. Metals lacking this mobility, by having internal microstructure that block dislocation motion, are usually brittle rather than ductile [10]. Figure (1) illustrate the contrasting fracture mechanics.

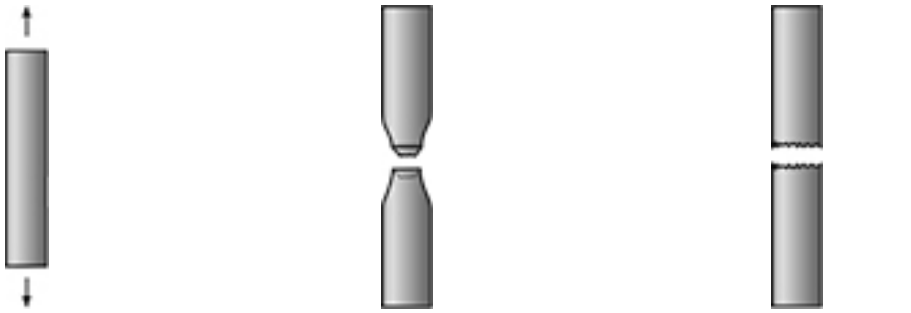

(a) Tensile forces (b) Ductile fracture (c) Brittle fracture

Figure 1: *Fracture of test specimens*

The stress generated by tensile forces is not quite uniform throughout the specimen, there will always be some locations where the local stress is at the maximum. For ductile metals, the increase in local stress accelerate plastic flow, causing *necking* in the gage length of the specimen. Until the neck forms, the deformation is essentially uniform throughout the specimen, but after necking all subsequent deformation takes place in the neck. The neck gets smaller and smaller until the high stress concentrations causes the specimen to fail. This will be the failure mode for most ductile metals, with a characterising *cup and cone* fracture [10]. Furthermore, in an engineers perspective, a ductile metal is usually considered to have failed when it has suffered elastic failure, i.e., when marked plastic deformation has begun. A brittle material cannot be considered to have definitely failed until it has broken, when the maximum tensile stress reaches the ultimate strength [9].

## 2.3 Analysis Methods

Analysing stress-strain relations in structural materials is essential in order to measure technological characteristics and to estimate mechanical properties of materials. The direct use of formulas for calculating stress and strain produced in the material is often considered inefficient. One then must resort either to numerical techniques such as the finite element method or to experimental methods. There has been a tremendous increase in the use of numerical methods over the years, but the use of experimental methods is still very effective. Many investigations make use of both numerical and experimental results to cross-feed information from one to the other for increased accuracy.

### 2.3.1 Experimental Method

The uniaxial tensile test may very well be the most useful material characterization test available. It works simply by continuously measuring the force required to elongate a test specimen by increasing increments until it fractures. The test measures a number of important material properties; elasticity, plasticity and ultimate strength. Most importantly, it generates stress-strain curves, which are an graphical measure of a material's mechanical properties. The curves are the unique identifiers of each material tested (material's DNA) [12]. Tensile tests carried out on ductile metals will usually generate stress-strain curves as illustrated in figure (2a), where the strain is specified as percentage.

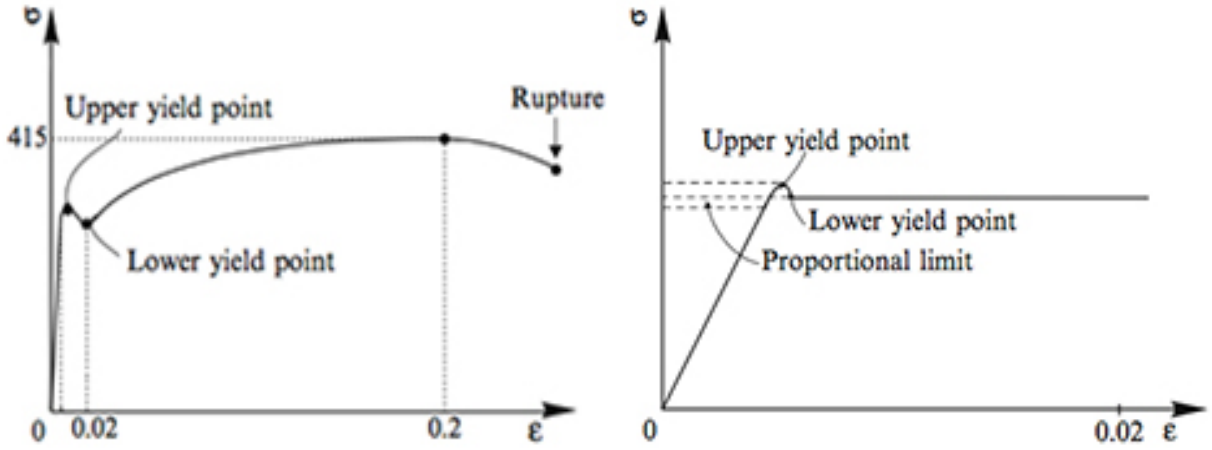


(a) Stress-strain diagram

(b) Expanded scale

Figure 2: *Stress-Strain diagram*

As a tensile test proceeds, the stress and strain increase linearly up to the proportional limit, as shown in figure (2b). The slope of the curve up to this point is known as the elastic modulus, or Youngs's modulus. The stress and strain reaches the upper yield point, or the elastic limit, where the behaviour of the metal switches form elastic to plastic. The nonlinear stress decreases to a lower yield, which represents the dislocations of atoms, before the stress increases up to a ultimate stress point. This region is known as strain hardening. Beyond the point of ultimate stress, the stress decrease as a result of necking, to a final fracture of the specimen.

If the stress (and therefore strain) applied to a material is lower than the elastic limit, both the stress and strain will return to zero if the load is removed. However, if the elastic limit is exceeded, only the elastic strain will be recovered, and the plastic strain will remain as permanent set. Since it is usually undesirable to experience permanent set in a component, engineers would like to design parts so that the expected service stress is less than the elastic limit by some reasonable factor of safety [12].

### 2.3.2 Numerical Method

There are great many numerical techniques used in stress-strain analysis for engineering applications. In the field of structural analysis, the most popular technique is the finite element method (FEM). This method is based on dividing a structure system into a finite number of smaller elements, which are interconnected at points (nodal points or nodes). Instead of solving the problem for the entire body in one operation, the finite element method formulate the

equations for each element and combine them to obtain the solution of the whole system. Analytical solutions given by mathematical expressions generally require the solution of ordinary or partial differential equations, which, because of complicated geometries, loadings, and material properties, are not usually obtainable. Hence we need to rely on numerical methods, such as the finite element method, for acceptable solutions. Briefly, the solution for structural problems typically refers to determining the displacements at each node and the stresses within each element making up the structure that is subjected to applied loads [13].

## 2.4 Mechanism of Heat Transfer

Thermodynamics provides the foundation for analysis of energy transformations involving heat, mechanical work and other aspects of energy. A thermal system is identified as the subject of the analysis, everything external to the system is considered to be part of the system's surroundings. The thermal systems involve the storage, transfer, and conversion of energy. Energy can be transferred between systems and its surroundings by work and heat transfer [8]. The $1^{st}$ law of thermodynamics state that the total amount of energy in an isolated system remains constant - energy can neither be created nor destroyed, it can only change forms. The $2^{nd}$ law of thermodynamics states that heat is energy transferred from one body to another by thermal interactions due to a temperature difference.

### 2.4.1 Conduction

The term *conduction* refers to the first mode of heat transfer. When a temperature gradient exists in a stationary medium, which may be solid or fluid, heat transfer occurs across the medium. The physical mechanism are defined by the activity of atoms and molecules transferring energy from the more energetic to the less energetic particles, due to oscillation and vibrations between the particles [8]. Higher temperature are associated with higher molecular movement, as the molecules collide a transfer of energy from the more energetic to the less energetic molecules must occur. The heat flux, or the heat transfer rate per unit area, is expressed with *Fourier's law* (6):

$$q_x = k \times \frac{dT}{dx} \tag{6}$$

Where $q_x$ is the heat flux$(W/m^2)$ and $k$ is the transport property, also known as the thermal conductivity $(W/m \times K)$, which is a characteristic of the material.

### 2.4.2 Convection

The second mode of heat transfer is termed *convection* and refers to heat transfer between a surface and a moving or stationary fluid, with different temperatures. The convection heat transfer mode is comprised of two mechanisms, energy transfer due to molecular motion, i.e. conduction, and macroscopic motion of the fluid [8]. There are two types of convection, forced and free convection. The former is a prosess where the fluid is circulated by external forces; the latter is when the flow is induced by buoyancy forces, which arise from density differences caused by temperature variation in the fluid. Regardless of the nature of the convection heat transfer process, the heat flux is expressed with *Newton's law of cooling* (7):

$$q = h \times (T_s - T_\infty) \tag{7}$$

Where $q_x$ is the heat flux$(W/m^2)$, which is proportional to the difference between the surface and fluid temperatures. The proportionality constant $h$ is termed the heat convection coefficient.

### 2.4.3 Radiation

The third mode of heat transfer is termed *radiation*. Unlike the two other heat transfer modes described; radiation does not require a medium to transfer heat between surfaces at different temperatures. In fact, radiation transfer occurs most efficiently in a vacuum [8]. Radiation is defined as energy *emitted* by matter that is at a finite temperature, and is transported by *electromagnetic waves*. The mechanism of emission is related to energy released as a result of oscillations or transitions of many electrons in the matter. The radiation heat flux, or the rate of energy released, is termed the surface *emissive power* and is expressed by *Stefan-Boltzmann law* (8):

$$E_b = \varepsilon \times \sigma \times T_s^4 \tag{8}$$

Where $E_b$ is the emissive power $(W/m^2)$, $\varepsilon$ is the *emissivity*, $\sigma$ is the *Stefan-Boltzmann constant* $(W/m^2K^4)$ and $T_s$ is the absolute temperature $(K)$ of the surface. The rate of energy released is highly dependent on the surface temperature, but also on the nature of the surface. This dependence is described by the emissivity, a dimensionless number between 0 and 1, representing the ratio of radiation from a particular surface compared to a ideal radiating surface, also known as a *black body*. Typical values of the total emissivity for selected materials are shown in figure (3).

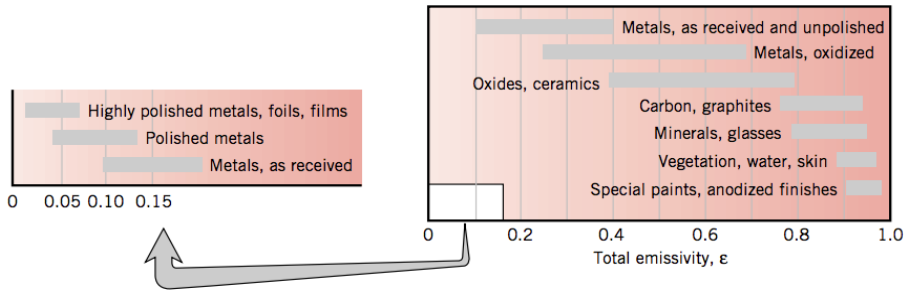


Figure 3: *Representative values of the total emissivity*

The complete electromagnetic spectrum, shown in figure(4), presents the different types of radiation based on wavelengths. The short wavelengths *gamma rays*, *X-rays* and *ultraviolet* radiation are primarily of interest to the high-energy physicist and the nuclear engineers, while the long wavelength *microwaves* and *radio waves* are of concern to the electrical engineer. The *thermal radiation* which includes a portion of *ultraviolet waves*, all the visible light and the *infrared waves*, are waves emitted by matter as a result of its temperature and is pertinent to the heat transfer [8].

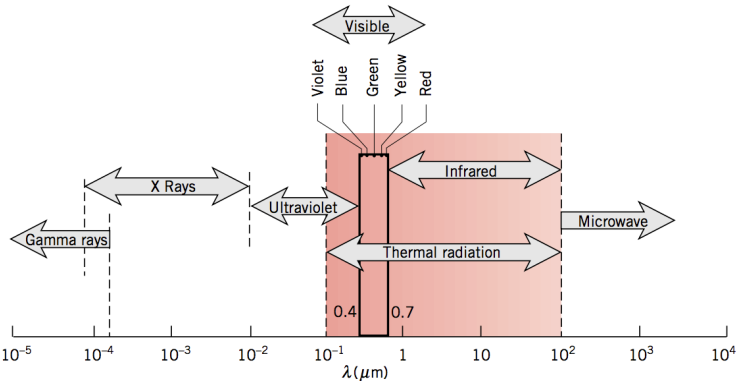


Figure 4: *Complete electromagnetic spectrum*

## 2.5 Thermography

The intermediate portion of the electromagnetic spectrum, presented in section (2.4.3), is categorised as the thermal radiation. These wavelengths extend from approximately 0.1-100$\mu m$, and is pertinent to heat transfer [8]. Only a small part of these electromagnetic waves, from 0,4 to 0,7$\mu m$, are visible to the naked eye as light. The wavelengths longer than the visible light are termed the infrared radiation. Thermography is a technique that exploits the infrared wavelengths of the electromagnetic spectrum, which the naked eye can't see. Much like a visible light camera, an *infrared camera* uses a lens to focus the infrared light of different wavelengths emitted by all object in view, which is converted into an electronic signal by infrared detectors. The signal is further processed digitally to create a thermal image. The working principle of thermography is illustrated in figure (5).

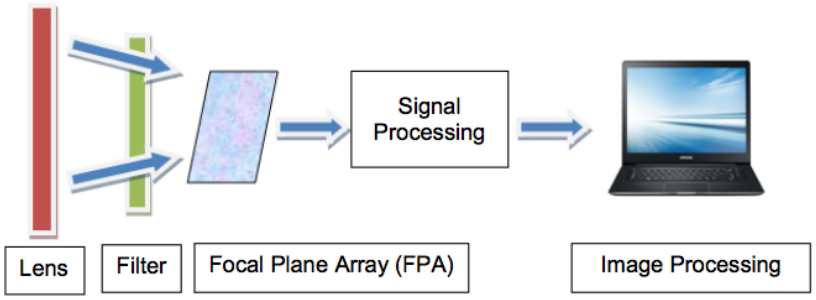


Figure 5: *Working principle of thermography*

## 2.6 Internal Friction

The phenomenon of *internal friction* - defined as the capacity of a vibrating solid to convert its mechanical energy of vibration into heat - differs from "friction" in the tribological sense, i.e., the resistance against the motion of two solid surfaces relative to each other [14]. In a solid material exposed to periodically varying stress, internal friction is most commonly manifested by the damping or loss of vibration amplitude, of a freely vibrating body, by some stress-strain hysteresis. A perfectly elastic material will not produce damping since, stress and strain are always in phase, and consequently no mechanical hysteresis or loss of vibrational energy can take place. Damping is, therefore, a result of the non-elastic behaviour of materials, and can

be observed at stress levels far below plastic flow [15]. In the approach to internal friction, which the present thesis is concerned, the origin and mechanism is in interest, rather than its desirability.

In most experiments investigating internal friction, the test specimens are subjected to a non-homogeneous strain. The elastic and non-elastic behaviour of the specimen is complicated by the dependence of stress and strain on position in the specimen. For a specimen with a non-elastic behaviour, homogeneous strain is to be assumed in a small element of a specimen within which the strain is uniform, or with a complete specimen throughout which the strain is the same at any instant.

### 2.6.1 The Thermoelastic Effect

The thermoelastic effect of a material is illustrated by the expansion of a solid when heated, and the reciprocal effect, the cooling during an adiabatic expansion. Stress applied to an element of material, will lead to an instantaneously strain by amount $\varepsilon'$, and accompanied by a change in temperature. If the applied stress is homogeneous, the same temperature change will occur throughout the specimen. On the other hand, a non-homogeneous stress applied will set up a temperature gradient in the material. The heat transfer into or out of the material produces an additional non-elastic strain. In general, a conversion of mechanical energy into heat will be a result of this heat transfer and the associated non-elastic behaviour [15].

The application of a periodically varying non-homogeneous stress will produce a time varying temperature gradient within an element of material. If the variation in stress are so rapid, i.e the frequency of the stress cycle are so high, that insufficient time is allowed for heat transfer to take place, the process is *adiabatic* and no energy loss, or damping, takes place. In stress cycles with sufficiently low frequencies, temperature equilibrium in the specimen is constantly maintained, or the process is *isothermal*. In the intermediate range of frequencies, where the conditions of application of stress are neither adiabatic nor isothermal, the conversion of mechanical energy into heat is not reversible and internal friction effects may be observed.

The thermoelastic effect may be investigated from two viewpoints. We may seek the rate of dissipation of the mechanical energy of vibration. This dissipation is due to the slight difference in phase between the stresses and the corresponding strains. On the other hand, we may seek the rate of heat generation. Stress inhomogeneities give rise to heat currents, which increase entropy, and an increase of entropy is inevitably associated with generation of heat [16].

# 3 Methodology

This chapter presents and discusses the experimental- and numerical methodology used in the study of this thesis. The procedures for the tests and simulations will be explained, with detailed overview of the equipments, softwares and raw-data acquisition. All the experimental tests has been carried out in the Safety Lab, and the numerical tests in the Computer Lab, at The Arctic University of Norway (UiT).

### Experimental Methodology

The uniaxial tensile test is usually carried out in room temperature with a short-time static loading (2.2.1), to determine material properties such as yield points, modulus of elasticity and ultimate strength. A *standard* testing temperature of $25°C$ is used because material properties change with temperature, of which Young's modulus increases when temperature decreases. The *standard* frequency of loading are considered to be sufficiently low, that temperature equilibrium in the test specimen is constantly maintained, i.e., the process is isothermal. This implies that energy entering the test specimen as work (W) must leave it again as heat (Q), done by heat transfer from the test specimen to the environment. For the study of this thesis, the uniaxial tensile test are performed in varying temperatures, with a frequency in the intermediate rage, where the conditions of applied stress are neither isothermal nor adiabatic. This allows us to observe changes in material properties and internal friction effects in the test specimens.

## 3.1 Tensile Testing

The tensile tests were conducted with the intentions of generating stress-strain diagrams and *infrared images* of the test specimens in varying temperatures, to observe changes in material properties and internal friction effects in the test specimens. The tensile tests was first carried out in room temperature ($25°C$), thereafter, the *Universal Material Tester* was moved into the *cold room* available in the Safety Lab. The cold room has been used for exposure of the tensile tests to low temperatures. For each defined temperature, the tensile test was carried out multiple times, in order to lower the uncertainties of the measurement results. Table (1) presents the selected testing temperatures and number of tensile tests performed for each defined temperature.

| | **Stress-Strain acquisition** | **Thermography monitoring** | **Total number of tests** |
|---|---|---|---|
| **Test** (25 $°C$) | 4 | 2 | 6 |
| **Test** (-5 $°C$) | 4 | 2 | 6 |
| **Test** (-10 $°C$) | 4 | 2 | 6 |
| **Test** (-15 $°C$) | 4 | 2 | 6 |
| **Test** (-20 $°C$) | 4 | 2 | 6 |
| | 20 | 10 | 30 |

Table 1: *Testing temperatures and number of tests*

### 3.1.1 Universal Material Tester

The universal material tester, displayed in figure (6), was used to carry out all the experimental tensile tests in this study. The material tester, and its associated equipment, are from the manufacturer *GUNT Hamburg*. The company delivers equipment for engineering education, and are developed specifically for experiments in small groups and is characterised by a clear design, simple operation and accessories that are easy to exchange. This universal material tester is capable of performing a wide range of material tests, but due to the study of this thesis, only the tensile test has been performed. The test procedure described on the company webpage:

*"The tensile specimens are clamped between the upper cross member and the crosshead. The test force is generated by means of a hand-operated hydraulic system and displayed on a large force gauge with drag indicator. A dial gauge measures the elongation of the specimens. The experimental unit can also be equipped with electronic force and displacement measurement. Using the WP 300.20 system for data acquisition, the measured values for force and displacement can be transferred to a PC where they can be analysed with the software"* [17].

Experiments:

- Tensile tests
- Plot stress-strain diagrams
- Brinell hardness test
- Compression tests
- Bending tests
- Cupping tests
- Shear tests
- Testing of plate and coil springs

Figure 6: *Universal Material Tester*

The advantage of using the simple equipment design in this study, with hand-operated hydraulic system, was the relatively light weight and that it did not require any power supply. The ability to easily move the equipment in and out of the cold room was essential to carry out the tensile test in low temperatures. On the other hand, the use of a manual hydraulic system offered challenges regarding the frequency of loading. Unlike automatic systems, where the frequency of applied stress are program controlled, the frequency of loading with the hand-operated hydraulic system is determined by the speed of *rotation*. All the tensile tests was carried out with a frequency of 5 seconds per rotation, resulting in a total test-time of 45-50 seconds. This frequency was considered to be as fast as reasonably possible, in order to maintain the same frequency from start to end.

### 3.1.2 Test Specimens

The test specimens used are from the same manufacturer as the universal material tester, *GUNT Hamburg* [18]. The company produce test specimens in various materials - steel, aluminium, copper and brass - which comply with the requirements of *DIN 50125*, the german standard for manufacturing of test specimens [19]. The material selected for this study was steel, with grade number *9SMn28* in the *DIN standard*, which is equivalent to grade number *11SMn30* in the *EU standard* [20]. The grade number indicates the chemical composition in the ferrous alloy. Table (2) presents the composition percentage for steel *9SMn28*:

| *Carbon* (C) | *Silicon* (Si) | *Manganese* (Mn) | *Phosphorous* (P) | *Sulfur* (S) |
|---|---|---|---|---|
| 0,00 - 0,14 | 0,00 - 0,05 | 0,90 - 1,30 | 0,00 - 0,11 | 0,27 - 0,33 |

Table 2: *Composition of steel 9SMn28 [weight-%]*

The steel specimen have a circular cross-section, with two centre punch marks on the shafts to mark the test length, as shown in figure (7). The number of tests performed for each defined temperature, presented in table (1), was determined with the consideration of test specimens at disposal. Priority was given to a greater amount of tests for each defined temperature, over a greater temperature range.

Figure 7: *Test specimen*

Technical data:

- Tensile specimens in acc. with DIN 50125
- Specimens diameter: 6mm
- Test length: 30mm
- Total specimen length: 64mm
- Attachment thread: M10
- Material: steel (9SMn28/11SMn30)

When mounting the test specimens to the material tester, it was tried to have as least possible physical contact with the test specimens. This was done to minimise the heat transfer to the test specimens, which increases the starting temperature of the tensile tests. However, the test specimens became difficult to mount to the material tester when carried out in the cold room, and some physical contact within the test length was necessary. Both the test specimens and the material tester was given sufficient time in the cold room at the defined temperatures to achieve the equivalent temperatures.

### 3.1.3 Data Acquisition

The universal material tester used was equipped with an electronic measuring system, in addition to the force gauge with drag indicator. The measuring system consists of a *pressure sensor* for force measurement, a *potentiometer* to measure the displacement and a measuring *amplifier* including a USB interface for connection to a computer [21]. By using this system, measured values for force and displacement can be transferred to a computer and analysed with the system software for data acquisition, *WP300.20*. Measured values are evaluated in the user-friendly software, so stress-strain diagrams can be recorded, saved and printed on a printer. Additionally, it is possible to print a complete test log, which is in accordance with DIN for tensile tests. Figure (8) illustrates the program window of the WP300 software with a completed recording.

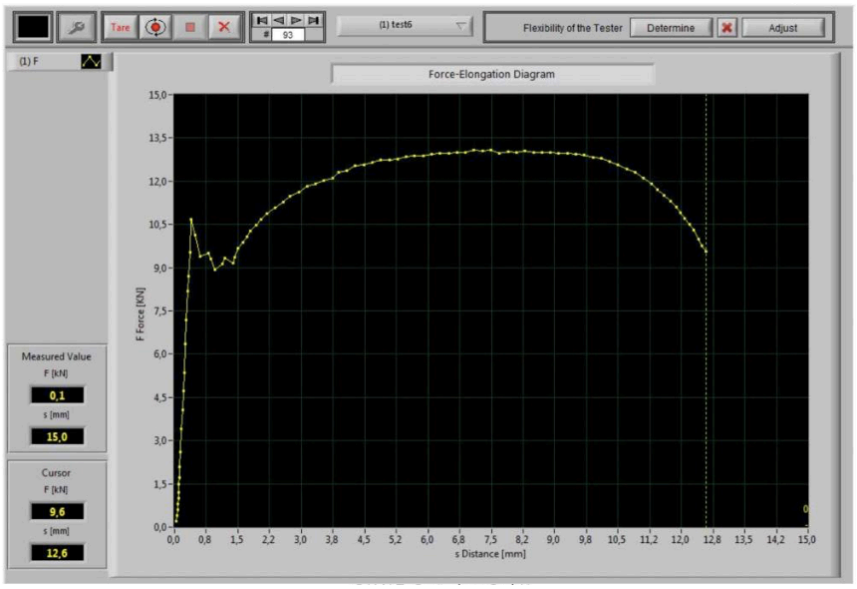


Figure 8: *WP300 Software-window*

The system software was installed on a laptop to record diagrams from the tensile tests carried out in the cold room. The laptop was placed right outside of the cold room, with the USB cable connected to the measuring amplifier stationed inside the cold room with the universal material tester. The cables connecting the pressure sensor and potentiometer to the amplifier was fairly short, making it impossible to place the amplifier outside the cold room. The only initial conditions in the software was to select the type of specimen to be tested, round or flat test specimen. Technical data such as the test length and cross-section area of the specimen was then automatically defined by the software. The force and elongation was reset to zero before starting the recordings. Figure (9) presents the raw data printed from the WP300 software.

| s [mm] | F [KN] | EPS [%] | SIGMA [N/mm^2] |
|---|---|---|---|
| 01:00:00,0 | 0,201 | 0,089 | 7,120 |
| 01:00:00,0 | 0,727 | 0,194 | 25,705 |
| 01:00:00,0 | 1,538 | 0,301 | 54,413 |
| 01:00:00,1 | 2,668 | 0,431 | 94,373 |
| 01:00:00,1 | 3,570 | 0,525 | 126,268 |
| 01:00:00,1 | 4,776 | 0,615 | 168,925 |
| 01:00:00,1 | 5,615 | 0,666 | 198,576 |
| 01:00:00,2 | 6,350 | 0,752 | 224,600 |
| 01:00:00,2 | 7,117 | 0,819 | 251,727 |
| 01:00:00,2 | 8,117 | 0,872 | 287,076 |
| 01:00:00,2 | 9,325 | 0,962 | 329,799 |
| 01:00:00,3 | 10,655 | 1,069 | 376,853 |

(a) *Printed test log*

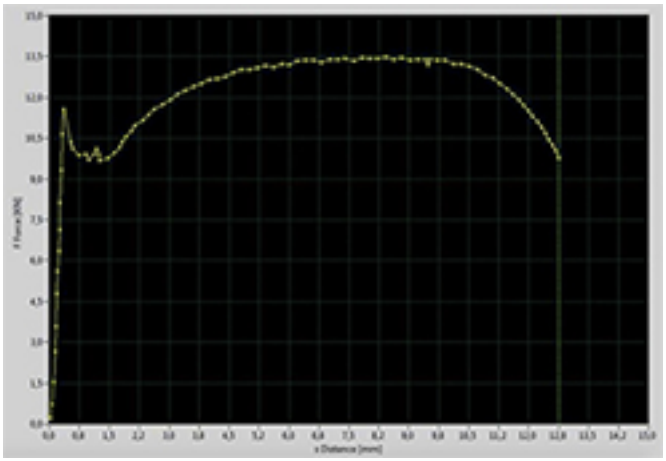

(b) *Printed stress-strain diagram*

Figure 9: *Raw data output*

The raw data was exported and stored for all tensile tests performed. The software was only capable of printing the data, i.e., exporting the diagram and test log as *pictures*. The complete test log, parts of which are illustrated in figure (9a), had to be manually rewritten into Excel for further data processing. A total of 20 complete test logs was printed, resulting in over 7200 numerical values to process. The stress-strain diagrams presented in the results were developed in excel, by the data from the printed test logs.

## 3.2 Thermography

The test specimens were monitored with thermography throughout the course of the tensile tests, to investigate the heat generation associated with the thermoelastic effects. By taking advantage of thermography, the infrared wavelengths emitted from the test specimen can be observed in high-definition thermal images. The rate of energy emitted as thermal radiation is highly dependent on the surface temperature. Small temperature changes in the test specimens will generate visible thermal signatures, readings of heat generation. As previously mentioned in section (2.4.3), the nature of the surface also has a impact on the emissive power. The total emissivity of unpolished metals, shown in figure (4), indicate a total emissivity of $0,1 - 0,4$. To increase the rate of energy emitted as thermal radiation, the unpolished steel specimens were coated with white paint, which has a much higher emissivity of $0,9 - 0,95$ [22]. The coated test specimen are illustrated in figure (13a).

### 3.2.1 Thermal Infrared Camera

The thermal infrared camera, displayed in figure (10), was used to monitor the test specimens in this study. The camera are from the manufacturer *FLIR Systems, Inc.*, a global leader within thermal imaging [23]. The company distributes innovative sensing technologies with a wide rage of application, from outdoor activities to military and defence. The *FLIR-T1030sc* model is designed for engineers, researchers, and scientists who need exceptional resolution and thermal sensitivity [24]. The camera is capable of recoding high-speed imaging and measurements in $1024 \times 768$ HD resolution at 30 frames per second. By using FLIR's *ResearchIR Max software*, the camera can be connected directly to the software, enabling for camera control, data recording, image analysis, and data sharing.


Figure 10: *FLIR-T1030sc*

Technical data:

- IR Resolution: 1024 × 768 pixels
- Emissivity Correction: variable from 0,1 to 1,0
- Detector Pitch: 17 $\mu m$
- Spectral Range: 7,5 $\mu m$ to 14$\mu m$
- Temperature Range: -40 $°C$ to +70 $°C$
- Accuracy: ± 1 $°C$ or ± 1% of reading

The camera was mounted on a tripod and stationed as near as possible to the universal material tester, without interfering with the hand operated hydraulic system. The field of view was manually adjusted, with a natural background to enhance the focus of the test specimen. Calibrations and image enhancement were performed in the software *ResearchIR Max*, before the recordings were started for each tensile test carried out. Based on the length of test time, the frame rate was specified to 1 frame per 5 seconds in the recording of the test specimens. This speed was considered to be fast enough to generate the desired thermal images, and producing a manageable amount of raw data to process.

### 3.2.2 Thermal Image Analysis

The thermal image analysis was performed in the software *ResearchIR Max*, the same software used for camera control and data recording throughout the course of the tensile tests. This software is highly customisable, with the ability to change parameters and enhance images recorded, to further analyse the images with spots, lines, and other measurement tools. The *Object parameters* are display as downloaded from the camera, where they can be override for more accurately computed temperatures of the object in display. The image enhancement tools allows control of scale limits and color distribution of the data. A histogram of the data is display for each image frame to visualise how the data values are distributed. This powerful tool can allow the user to see amazing detail even in low contrast imagery [25]. Figure (11) illustrates the main window of FLIR's ResearchIR software.

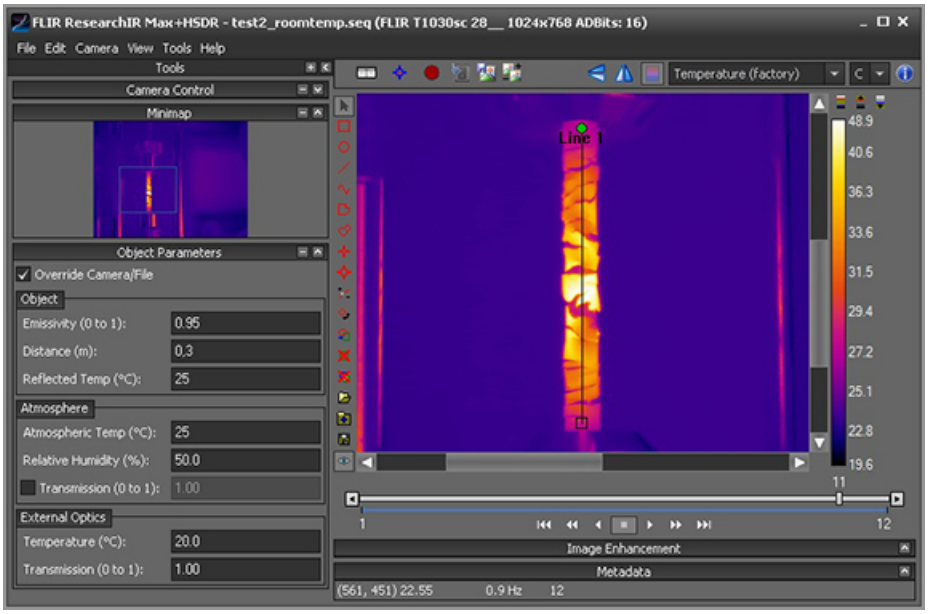


Figure 11: *FLIR Research software-window*

The object parameters were adjusted for each recording analysed. The emissivity was defined to 0,95 for all analysis, in accordance to the white coating of the test specimen. Reflected- and atmospheric temperature were changed to the defined testing temperatures of recording. The analysis tools available in the software allows the user to draw a *Region of Interest* (ROI) using a variety of drawing tools. The test specimens was analysed with the *Line ROI*, which draws a straight line of interest as shown in figure (11). The data along the selected ROI can be presented in a *profile plot*, which creates a X-Y graph of the temperature data versus pixels along the ROI. The profile plot can be exported from the software, including both raw data and the graph, as presented in figure (12).

| Pixel | Line 1 |
|---|---|
| 1 | 2.713939e+01 |
| 2 | 2.715977e+01 |
| 3 | 2.690817e+01 |
| 4 | 2.692859e+01 |
| 5 | 2.680600e+01 |
| 6 | 2.679237e+01 |
| 7 | 2.681281e+01 |
| 8 | 2.681963e+01 |
| 9 | 2.688093e+01 |
| 10 | 2.703744e+01 |

(a) *Exported data*

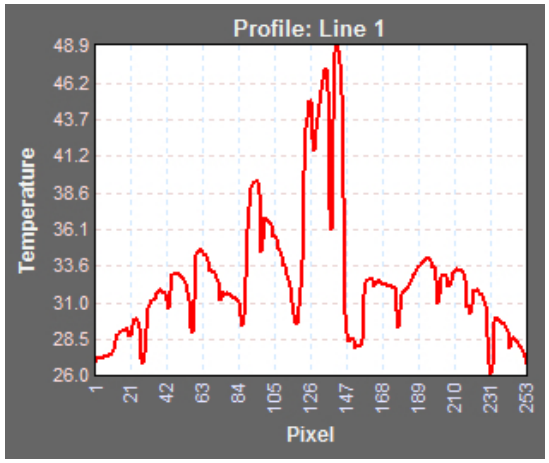


(b) *Exported graph*

Figure 12: *ROI - Profile plot*

The profile plot was exported for all the tensile tests performed with thermography monitoring. The exported raw-data required some modifications in excel, where the X-Y values were presented in one column, as shown in figure (12a). Further data processing was performed to convert the X-axes from pixels to millimetres, by using the known test length and elongation of the test specimens. The profile plot of the test specimen, as shown in figure (12b), indicates an irregular distribution with substantial temperature drops. This uneven distribution is caused by cracking in the coating of the test specimen, which clearly visualise the difference in energy emitted from the white paint and unpolished steel. An estimated temperature distribution were created by only using the peak-values in the profile plot. Figure (13) shows the coated test specimen before and after fracture.

(a) *Before*

(b) *After fracture*

Figure 13: *Coated Test Specimen*

### 3.3 Numerical Analysis

The main focus for the study of this thesis was to carry out the experimental tensile tests in defined temperatures, to analyse the material changes and internal friction effects that may occur in the test specimens. In addition to this objective, a numerical analysis was performed qualitatively for the tensile test, to visualise the procedure and results that are possible to achieve from this analysis method. The numerical analysis was performed in the software *ANSYS Workbench*, a simulation platform for performing structural, thermal and electromagnetic analyses [26]. In its most basic use, the ANSYS workbench process is straightforward: you select the type of analysis you wish to perform from the analysis systems, and you work through the cells in the system, generally from top to bottom, until you have completed all the required steps for your analysis [27]. The analysis system used for the tensile test are shown in figure (14), with the following analysis approach:

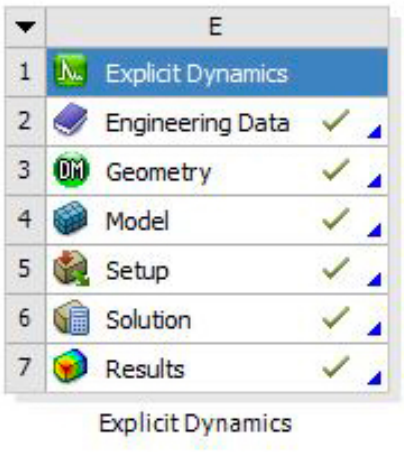


Figure 14: *Analysis system*

Analysis approach

1. Select analysis method
2. Define material properties
3. Create geometric model
4. Generate finite element mesh
5. Define loads and support
6. Solve the model
7. View the results

The analysis method selected for the tensile test was *Explicit dynamics*, an nonlinear approach for structures exposed to short-duration severe loading, large material deformation and material failure [28]. By using this analysis method, the plastic behaviour can be observed, with mechanisms as necking and fracture of the test specimen. Material properties used in explicit dynamic analyses require data table input, a series of constants that are interpreted in the simulation. As a result of unavailable material data for steel 9SMn28, the numerical analysis was carried out with a predefined material, available in the engineering data. The material selected was *Carbon Steel Grade 1006*, which had the most similar properties as the steel used in the experimental tests. The composition of the Carbon Steel is presented below [29]:

| *Carbon* (C) | *Manganese* (Mn) | *Phosphorous* (P) | *Sulfur* (S) |
|---|---|---|---|
| 0,080 | 0,25-0,40 | 0,040 | 0,050 |

Table 3: *Composition of 1006 Carbon Steel [weight-%]*

Creating the design model of a structure to be analysed is the first step in the simulation process. The geometry can be created from scratch in the *DesignModeler* (DM), which is a component of ANSYS Workbench, or an existing geometry can be imported into the software. The test specimen was created from scratch, with the dimensions presented in section (3.1.2). A small notch was made in the middle of the test length to define the location of desired fracture. By taking advantage of symmetry, only one-quarter of the test specimen was necessary to model, as presented in figure (15a). The next step in the simulation process was to define a high-quality mesh for the structure, a critical requirement for efficient and accurate explicit analysis. The method of meshing selected for the test specimen was the *Patch Conforming Method*, which gave a total of 4150 nodes and 19283 elements. The model of the test specimen with meshing is shown in figure (15b).

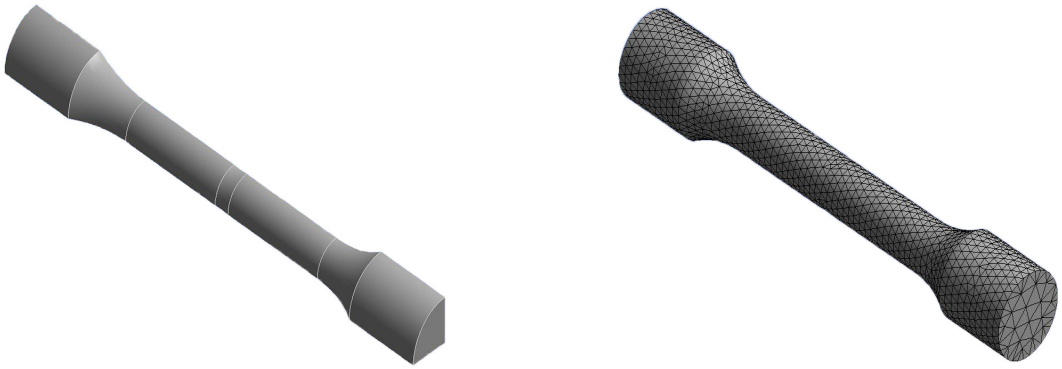

(a) *Geometric model* (b) *Finite element mesh*

Figure 15: *Tensile specimen*

The following step in the analysis approach was to define the loads and support, boundary conditions, and otherwise configure the analysis settings. Initially, the aim was to simulate the tensile test in the same conditions as done for the experimental tensile tests, by defining a load with velocity (elongation per second) and a total test time of 50s in the analysis settings. However, because of limitations to short-duration loading, the desired frequency was not possible to use in the explicit dynamic analysis. The load had to be defined as displacement, with a very short test time, for the simulation of the tensile test to be successful. The numerical analysis are based on a simulation performed with a displacement of $16mm$, and a defined test time of $0,001seconds$. Figure (16) shows the fixed support and displacement of the test specimen.

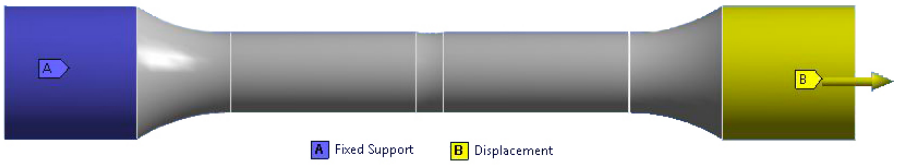


Figure 16: *Load and support*

The last steps of the analysis approach was to solve the model and view the results. The software is capable of many solver outputs, of which the stress and temperature were in interest for this analysis. The test specimen was solved for *equivalent (Von-Mises) Stress*, and for temperature by *user defined results*. Due to the defined test time, the tensile test was simulated with a significant load under adiabatic conditions. The resulting data was, therefore, not comparable with the data from the experimental tensile tests. Disregarding the data outputs, the simulation visualises the stress concentrations and heat generation in the test specimen, which has been analysed and compared qualitatively with the experimental tests. Figure (17) shows the software-window of the explicit dynamic analysis in ANSYS Workbench.

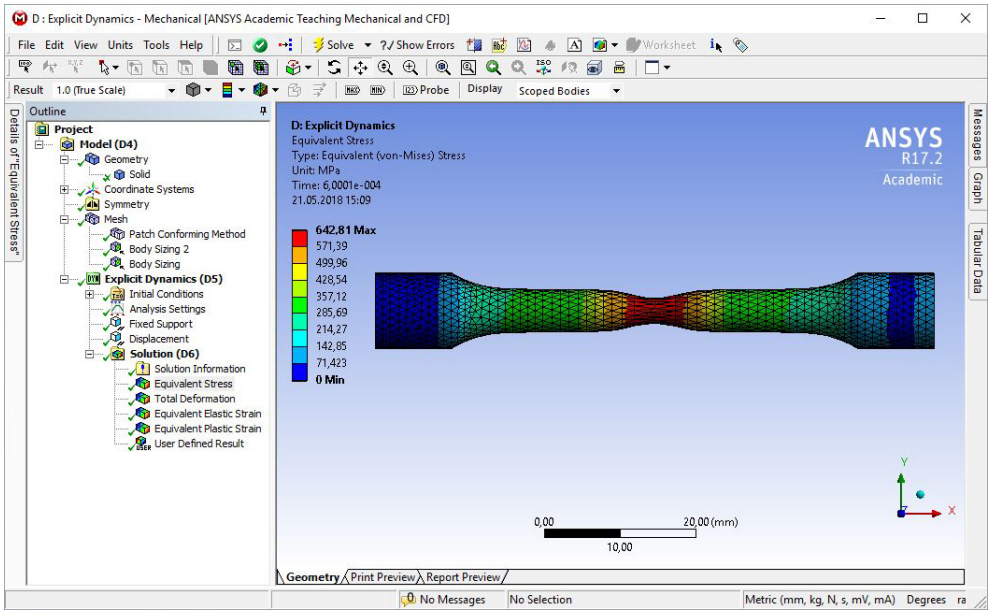


Figure 17: *Ansys Workbench software-window*

# 4 Results and Discussion

This section presents, and discuss, the analysis results of the experimental- and numerical tests performed in this study. Due to the large amount of processed data, the test results for each defined temperature are presented in the appendix, and referred to in the discussion of each analysis. The section is divided into subsections by the different analysis, directly related to the objectives stated in the introduction.

1. Stress-strain analysis: Study the change in steel properties with varying temperature
2. Thermography analysis: Study the internal friction effects in steel
3. Numerical analysis: Qualitative comparison with the physical experiments

## 4.1 Stress-Strain Analysis

The room temperature tensile behaviour exhibited by the steel specimen was typical of that expected from ductile materials, as illustrated in figure (2). That is, the initial region exhibited an linear response of stress and strain, followed by a region of work hardening to a ultimate strength, and finally a region of decreasing stress to final fracture of the specimen. The generated stress-strain digram for the tensile tests carried out in room temperature (25 $°C$) are presented in figure (18). By observing the diagram, the response of stress and strain are varying, to a certain extent, for each test performed. The measured stress values of interests, upper yield and ultimate strength, indicate a standard deviation of 20 $N/mm^2$ and 11 $N/mm^2$ representatively. This is a reasonable large difference, of tensile tests carried out in the same conditions, with an equal frequency. For analysing the change in stress relations with decreasing temperature, average stress values should be used for each defined temperature.

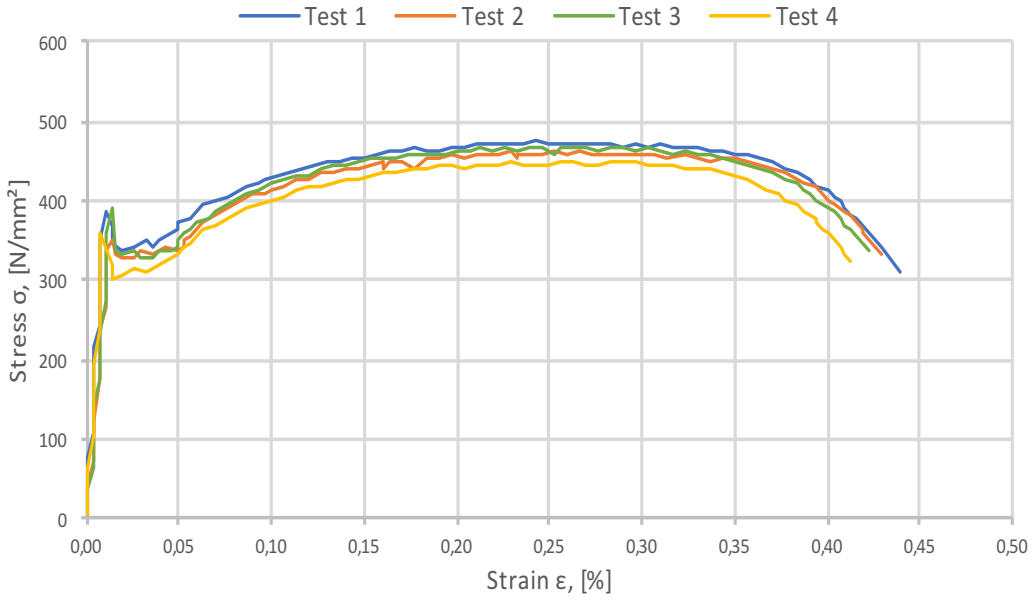


Figure 18: *Stress-Strain diagram (+25°C)*

The measured yield- and ultimate stress values for all room temperature tests are presented in table (4). As seen from the table, the calculated average values indicate a yield stress of 370 $N/mm^2$, and a ultimate stress of 462 $N/mm^2$. By comparing these average stress values with specification sheets, we can verify the analysis approach and validity of the results. Stated mechanical properties for $9SMn28$ steel indicates a yield stress of 375 $N/mm^2$ and a tensile stress (ultimate stress) of 460-710 $N/mm^2$ [30]. The measured room temperature properties are, according to the specification sheet, approximately equal for the yield stress and within the range of ultimate stress.

| | **Yield Stress** ($N/mm^2$) | **Ultimate Stress** ($N/mm^2$) |
|---|---|---|
| **Test 1** | 384,31 | 474,21 |
| **Test 2** | 348,03 | 460,88 |
| **Test 3** | 389,89 | 466,11 |
| **Test 4** | 358,91 | 447,93 |
| **Average** | 370,29 | 462,28 |

Table 4: *Stress values* ($+25°C$)

The generated stress-strain diagrams, with tables of associated stress values, are presented for all test temperatures in appendix (A). The characteristic upper- and lower yield points, ultimate strength, and fracture point are all presented in the tables, with it's calculated average values. Figure (19) presents the stress-strain diagram, with average stress values for each defined temperature.

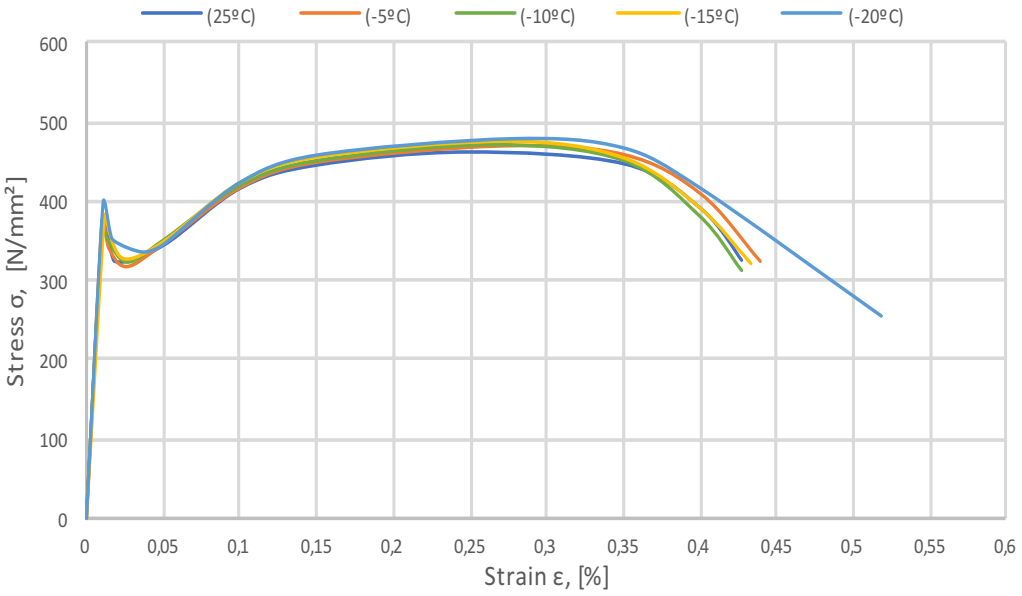


Figure 19: *Average stress-strain diagram*

The average stress-strain diagram indicate an approximately equal tensile behaviour for all temperatures, with the region of necking in -20 $°C$ as an exception. The fracture are each tests fingerprint, as they are all unique, and will not be compared with the defined temperatures. To observe the stress points of interest, one may need to study the expanded scales of the stress-strain diagram, as presented in figure (20). The average stress-strain curves indicates a minor increase in both yield- and ultimate stress, with decreasing temperature.

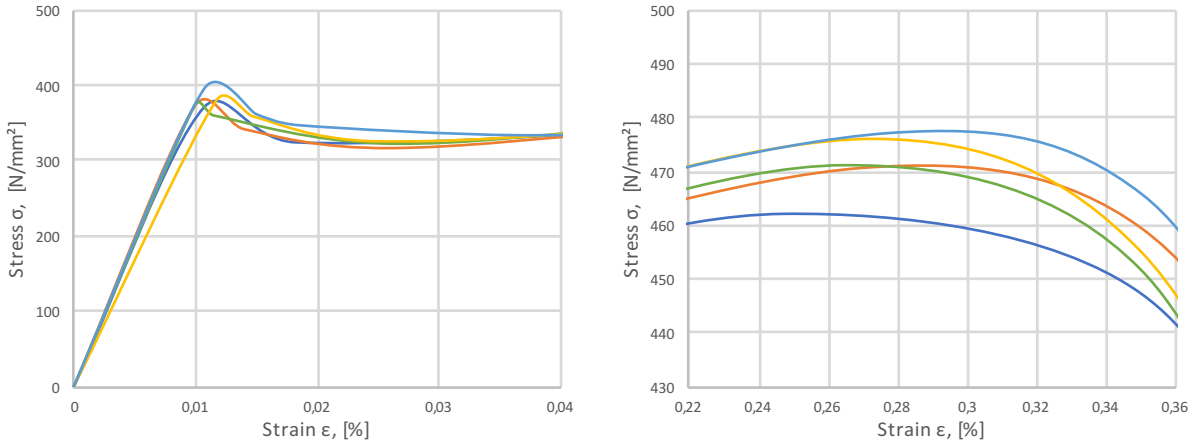


(a) *Yield Stress* (b) *Ultimate Stress*

Figure 20: *Expanded scales*

The average values for yield stress and ultimate stress are presented in table (5), with the calculated standard deviation. The yield stress exhibited an increase of 26 $N/mm^2$, where the largest jump in stress occurred from -15 $°C$ to -20 $°C$. The ultimate stress exhibited a total increase of 15 $N/mm^2$, with a steady increase between -5 $°C$ and -20 $°C$. The standard deviation of the average yield stress indicate the highest uncertainty for room temperature and -5 $°C$. The average ultimate stress indicate a reasonable low uncertainty for all test temperatures.

| | **Yield Stress** ($N/mm^2$) | **Ultimate Stress** ($N/mm^2$) |
|---|---|---|
| **Test (25 $°C$)** | 370,29 ± 10,02 | 462,28 ± 5,514 |
| **Test (-5 $°C$)** | 374,30 ± 8,07 | 470,63 ± 2,62 |
| **Test (-10 $°C$)** | 375,26 ± 3,51 | 471,29 ± 2,69 |
| **Test (-15 $°C$)** | 381,80 ± 4,26 | 476,17 ± 4,38 |
| **Test (-20 $°C$)** | 396,54 ± 5,24 | 477,37 ± 1,46 |

Table 5: *Average stress values*

Based on the results from the average stress-strain diagram and table of associated stress values, the observed change in material properties of $9SMn28$ steel, in the defined temperature range, can be interpreted as insignificant. Due to unavailable data of mechanical properties in low temperatures, the measured properties can't be compared with specification sheets. However, the general behaviour of steel at low temperatures, as illustrated in figure (21), can verify the results from the experimental tensile tests. The yield stress (Y.P.) and ultimate stress

(T.S.) curve indicate a minor increase in stress within the selected temperature range, from 25 $°C$ to - 20 $°C$. In addition, the yield curve indicate a larger increase versus the ultimate curve, which correspond with result of the experimental tensile behaviour.

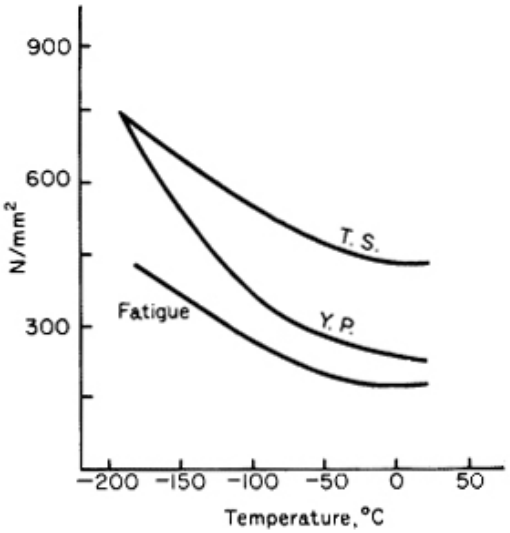


Figure 21: *Steel behaviour at low temperatures*

## 4.2 Thermography Analysis

The heat generation exhibited in the steel specimens was of that expected, with neither isothermal nor adiabatic conditions of applied stress. That is, the mechanical energy entering the test specimen, in form of applied stress, converted into heat, or internal friction. The steel specimen exhibited the same temperature change throughout the specimen in the initial phase, as the applied stress was homogeneous. Following, a temperature gradient developed in the specimen, as a result of the non-homogeneous stress in the plastic region. The same behaviour was observed for all defined temperatures. Figure (22) presents the thermal images recorded of a tensile test performed in -20 $°C$, illustrating the heat generation in the steel specimen as a result of the applied stress. The first frame illustrate the steel specimen in the start of the tensile test, right before the stress was applied, indicating an approximately equal temperature as its surroundings. The increase in temperature are noticeable for each frame recorded, with the development of a temperature gradient, until final fracture of the specimen.

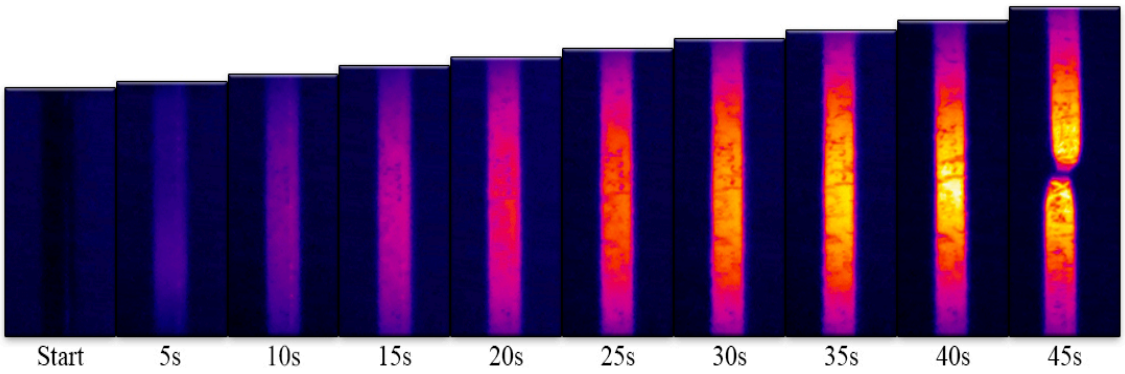


Figure 22: *Heat Generation (frame 1-10)*

The highest increase in temperature was, as expected, recorded in the second last frame for all tensile tests, before fracture of the steel specimen. This frame represents the point of maximal stress concentrations, which convert into heat, or internal friction. To study the heat generation in the steel specimens, the temperature difference from start to end are of interest. The end state are further defined as the last frame before fracture. Figure (23) presents the thermal images of the first test in room temperature, where (23a) shows the start temperature and (23b) the end temperature of the test specimen. In contrast from the thermal images shown in figure (22), a heated plate was used in the background of the specimen. By analysing the thermal images, with associated colour bars, the steel specimen indicate a start temperature of around 25 $°C$, and a maximum end temperature of around 50 $°C$. As this test had a total test time of 50 seconds, the end temperature was observed at 45 seconds.

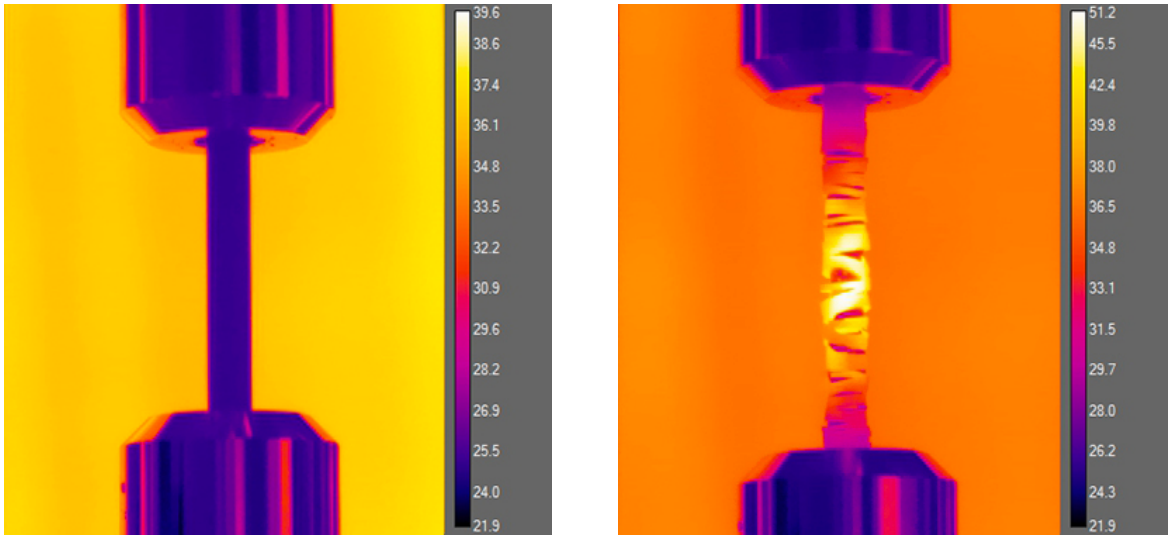


(a) *Start* (b) *End (45s)*

Figure 23: *Thermal image of steel specimen (*25$°C$)

The following profile plots of the thermal images are presented in figure (24). The temperature distribution in the steel specimen at start (24a) indicates an insignificant variation in temperature. The drop in temperature for both ends of the steel specimen indicate heat transfer influenced by the material tester. The average start temperature was calculated to 24,22 $°C$, which are illustrated with the orange horizontal line. The profile plot of the end temperature (24b) indicate a typical bell curve distribution, with a maximum temperature in the middle and decreasing temperature towards the ends of the steel specimen. A variation of 22 $°C$ can be observed in the steel specimen, with a maximum temperature of 50,3 $°C$, on top of the bell curve. The analysis of the thermal images, with associated colour bars, gives very accurate readings of the temperature in the steel specimen, compared with the profile plot. The temperature difference in the steel specimen, from start to end, are approximately 26 $°C$.

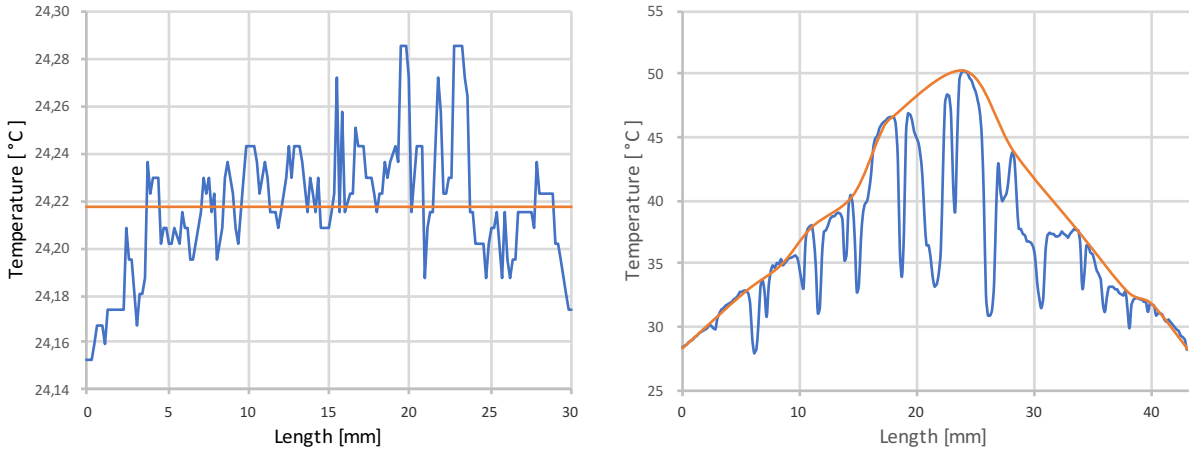


(a) *Start* (b) *End (45s)*

Figure 24: *Temperature distribution (25°C)*

The profile plots for all tensile tests are presented in appendix (B). The start distribution indicated a higher variation for some steel specimen at low temperature, which can be interpreted as heat transfer to the specimen and influence of the material tester. The profile plot for all end temperatures exhibited the same bell curve distribution, to a certain extent. The profile plot of test 1 (-20 $°C$), presented in appendix (B.5), shows the *real* temperature distribution in the steel specimen, as the coating did not crack. Table (6) presents the values of interests from the profile plots, for each defined test temperature:

| | | **Start** ($T_1$) | **End** ($T_2$) | $\Delta T$ |
|---|---|---|---|---|
| **Test** ($25°C$) | **1.** | 24,218 | 50,3 | 26,083 |
| | **2.** | 23,059 | 49,2 | 26,141 |
| **Test** ($-5°C$) | **1.** | -8,614 | 14,292 | 22,906 |
| | **2.** | -8,9367 | 13,84 | 22,777 |
| **Test** ($-10°C$) | **1.** | -16,827 | 12,104 | 28,931 |
| | **2.** | -16,554 | 11,279 | 27,832 |
| **Test** ($-15°C$) | **1.** | -17,356 | 8,077 | 25,433 |
| | **2.** | -17,428 | 5,015 | 22,442 |
| **Test** ($-20°C$) | **1.** | -25,623 | 0,486 | 26,109 |
| | **2.** | -24,888 | 0,215 | 25,102 |
| **Average** | | | | 25,376 |

Table 6: *Temperature values*

The results of the infrared images and associated profile plots indicate an approximately equal heat generation in the steel specimen, for all defined test temperatures. The temperature difference in the specimen varies for each test temperature, but not in a specific pattern. The minimum temperature difference observed was 22,44 $°C$, and a maximum difference of 28,93 $°C$. The calculated standard deviation indicate an uncertainty of 2,2 $°C$, which are insignificant. Based on these results, the heat generation in the steel specimen can be determined by the average increase in temperature, which equals 25,4 $°C$.

### 4.3 Numerical Analysis

By using the Finite Element Method, the displacement at each node and the stresses within each element could be observed with the applied loads. The simulated tensile test of *1006 Carbon Steel* in the explicit dynamics analysis are presented in figure (25). The test specimen exhibited an approximately equal tensile behaviour as of that observed from the physical experiments. The initial region indicated evenly distributed stress in the test length, which gradually converted into stress concentrations, followed by necking and final fracture of the specimen. The ultimate stress was observed just before the start of necking, which corresponds with the experimental tensile test. A deviation with the numerical analysis may be interpreted as the early start of necking. Further, the failure mode was relatively equal to the characteristic cup and cone fracture, which was observed for all experimental tensile tests.

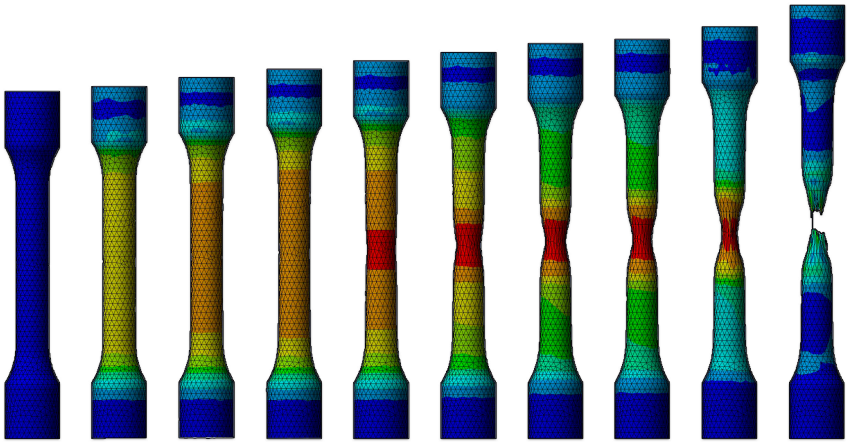

Figure 25: *Numerical tensile test*

Figure (26) presents the stress curve generated from the simulated tensile test. The equivalent stress is plotted versus test time, and indicate a immediate resemblance to the stress-strain curves generated from the experimental tensile test. The stress curve exhibit an equal initial region, with linear response of stress, followed by a upper yield point. The difference can be observed in the region of work hardening, where the stress curve is generated without a lower yield point. This is a result of software limitations, as the material behaviour in this region are not possible to simulate in the explicit analysis. The point of ultimate stress can be observed in the stress curve, followed by necking and a decrease in stress. A deviation of the stress curve can be observed in the concluding region, where the specimen fractures. The increase in stress are caused by high calculated stress values in the fracture elements in the specimen. Considering the stress points of interest, upper yield- and ultimate strength, the numerical stress curve correspond with the generated experimental stress-strain diagrams.

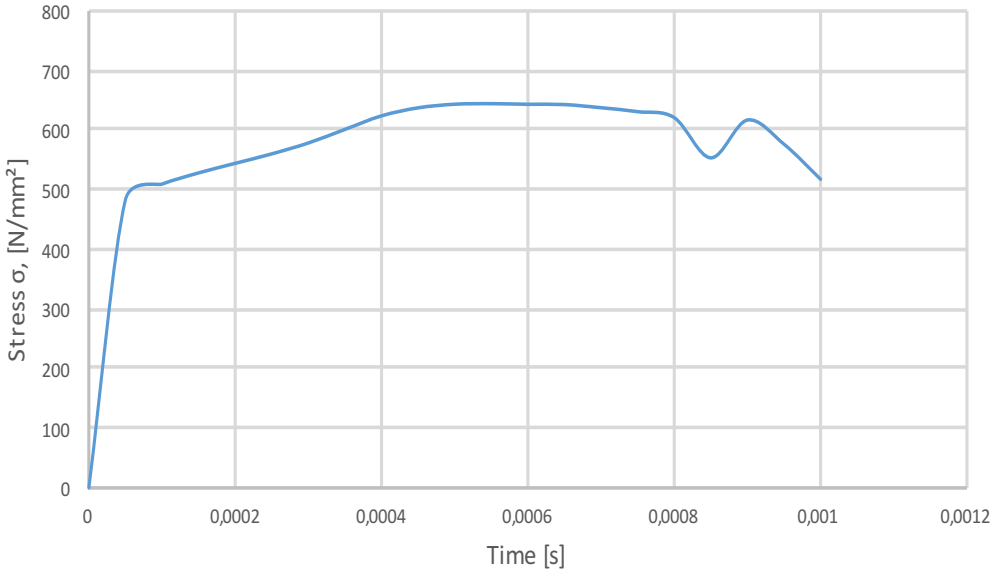


Figure 26: *Numerical stress curve*

Figure (27) presents the temperature distribution in the test specimen at the time of maximum stress concentrations, before fracture. The diagram are generated by *user defined temperature result*, which calculated the temperature in the test length of the specimen, based on the equivalent stress values. The numerical temperature distribution present a fairly similar curve as to the bell curve generated in the profile plots of the experimental tensile tests. That is, a maximum temperature in the middle, which decreases towards the ends of the test specimen. As the tensile test was simulated with adiabatic conditions, no significant time was given for heat transfer to take place. This is visualised by the concentrated heat generation in the middle of the test specimen.

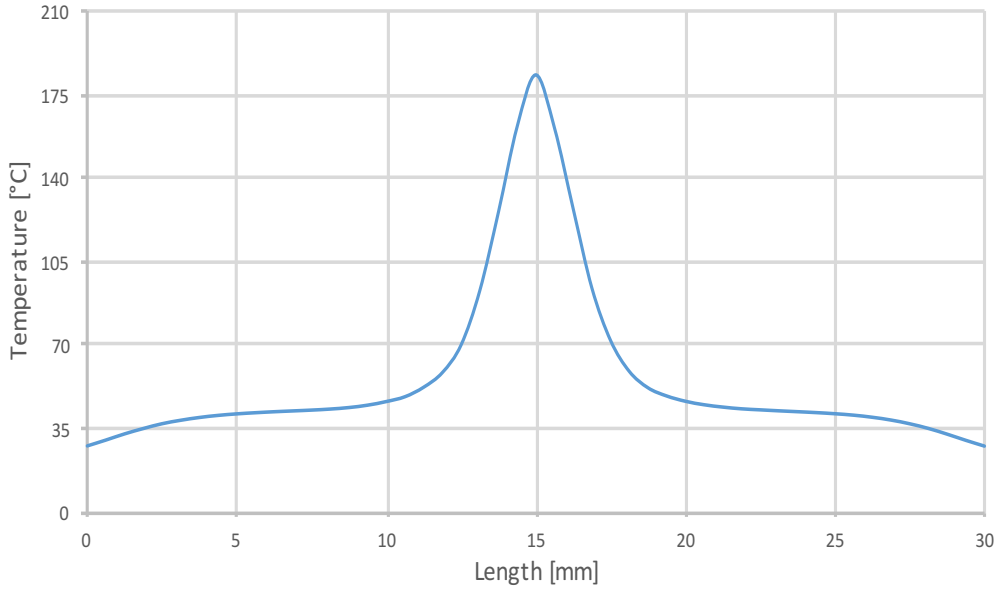


Figure 27: *Numerical temperature distribution*

# 5 Summary and Conclusion

The steel 9SMn28 exhibited a ductile behaviour for all test temperatures, with definite yield points and considerable ultimate elongation. From the generated stress-strain diagrams, a change in material properties could be observed, with decreasing temperature. The yield stress exhibited an increase of 26 $N/mm^2$, and the ultimate stress an increase of 15 $N/mm^2$. These results correspond with the general behaviour of steel, in the defined temperature range from 25 $°C$ to -20 $°C$. For engineering design studies, the observed change in steel properties can be interpreted as is insignificant within this temperature range. Lower temperatures is needed for concerns of brittleness in steel, i.e., increase in yield- and ultimate stress.

Heat generation, associated with the thermoelastic effects, could be observed in the steel specimen with thermography. From the generated profile plots, a typical bell curve temperature distribution developed, as a result of the stress concentrations in the steel specimens. The heat generation was approximately equal for all defined test temperatures, with an average temperature increase of 25,4 $°C$. The tensile tests were carried out with an equivalent frequency, which indicate an approximately equal energy entering the test specimen as work for all tests performed. As the total amount of energy remains constant, an equal transformation of energy must occur in the steel specimen. To observe changes in heat generation, a variation in frequency could be used, instead of atmospheric temperature.

The finite element method looks to be a valid approach for generating graphical measures of mechanical properties and heat generation in the test specimen. The generated stress curve indicated an relatively equal behaviour as that observed from the experimental stress-strain curves. Important material properties, as the yield point and ultimate strength, could easily be determined from the stress curve. The numerical temperature distribution indicated a fairly similar curve to the bell curve distribution generated from the profile plots, considering the simulation conditions. The accuracy of the explicit solution could be verified only via quantatively comparison with physical experiments.

# 6 Further work

The presented analysis in this thesis can be improved with a few suggestions of future work:

- Perform tensile tests in a greater temperature range, with an increased accuracy of frequency. The amount of tests for each defined temperature can be increased, to lower the uncertainty even more. Analyse the change in properties for different materials with decreasing temperature.
- Perform thermographic monitoring of steel specimens in a greater temperature range, to observe the heat generation with a significant change in material properties. The heat generation can be observed and compared for different materials. Associate the heat generation and bell curve distribution with equations.
- A numerical analysis could be performed quantitatively, with varying temperatures.

## References


[1] K. D. Piyush, "Behavior of material at cold regions temperatures," *US Army Corps of Engineers*, 1988.

[2] N. Dalette, "Failure literacy in structural engineering," *Elsevier Ltd.*, 2009.

[3] T. Foecke, "Metallurgy of the rms titanic," *U.S. Department of Commerce*, 1995.

[4] E. R. Parker, *Brittle behavior of engineering structures.* New York, John Wiley and Sons, Inc., 1957.

[5] T. H. G. Megson, "Structural and stress analysis," *Butterworh-Heinemann*, 1996.

[6] H. Young and R. Freedman, *Sears and Zenabsjy's University Physics.* Jim Smith, 2012, vol. 1.

[7] R. Janco and B. Hucko, *Introduction to Mechanics of Materials.* Bookboon, 2013.

[8] M. Moran, H. Shapiro, B. Munson, and D. DeWitt, *Introduction to thermal systems engineering.* John Wiley and Sons, 2003.

[9] W. C. Young and R. G. Budynas, *Roark's Formulas for Stress and Strain.* McGraw-Hill, 2002.

[10] D. Roylance, *Mechanical properties of materials.* MIT, 2008.

[11] P. Kelly. Mechanics lecture notes: An introduction to solid mechanics. [Online]. Available: http://homepages.engineering.auckland.ac.nz/~pkel015/SolidMechanicsBooks/index.html

[12] M. Gedeon, "Stress-strain concepts," *Materion Brush Performance Alloys*, 2012.

[13] D. L. Logan, *Finite Element Method.* Cengage Learning, 2012, vol. 5.

[14] M. Blanter, I. Golovin, H. Neuhäuser, and H.-R. Sinning, *Internal Friction in Metallic Materials.* Springer-Verlag Berlin Heidelberg, 2007.

[15] A. Nowick, "Internal friction in metals," *Progress in Materials Science*, vol. 4, pp. 60–62, 1953.

[16] C. Zener, "General theory of thernoelastic internal friction," *Internal Friction in Solids*, vol. 53, pp. 90–99, 1938.

[17] Universal material tester. [Online]. Available: https://bit.ly/2IoV0TI

[18] Tensile specimen. [Online]. Available: https://bit.ly/2JZZUnz

[19] M. T. S. Committee, "Testing of metallic materials - tensile test pieces," *DIN 50125*, 2004.

[20] (2011-2018) European steel and alloy grades. [Online]. Available: http://www.steelnumber.com/en/steel_composition_eu.php?name_id=155

[21] System for stress-strain acquisition. [Online]. Available: https://bit.ly/2IhH4ep

[22] Emissivity of comman materials. [Online]. Available: https://www.omega.com/literature/transactions/volume1/emissivityb.html

[23] Flir systems, inc. [Online]. Available: http://www.flir.eu/aboutFLIR/

[24] (2015) Flir-t1030sc. [Online]. Available: https://www.flir.com/globalassets/imported-assets/document/t1030sc-brochure-web-version.pdf

[25] Researchir user's guide. [Online]. Available: https://assets.techedu.com/assets/1/26/FLIR_ResearchIR_User_Manual1.pdf

[26] Engineering simulation platform. [Online]. Available: https://www.ansys.com/products/platform

[27] *ANSYS Workbench User's Guide*, ANSYS, Inc., 2009.

[28] (2011) Explicit dynamics. [Online]. Available: https://www.ansys.com/-/media/ansys/corporate/resourcelibrary/brochure/ansys-explicit-dynamics-brochure-140.pdf

[29] Carbon steel grade 1006. [Online]. Available: http://elginfasteners.com/resources/materials/material-specifications/carbon-steel-grade-1006/

[30] Ju feng special steel co., ltd. [Online]. Available: https://www.jfs-steel.com/en/steelDetail/DIN-9SMn28/DIN-9SMn28.html

# A Stress-Strain Results

## A.1 Stress-Strain diagram ($+25°C$)

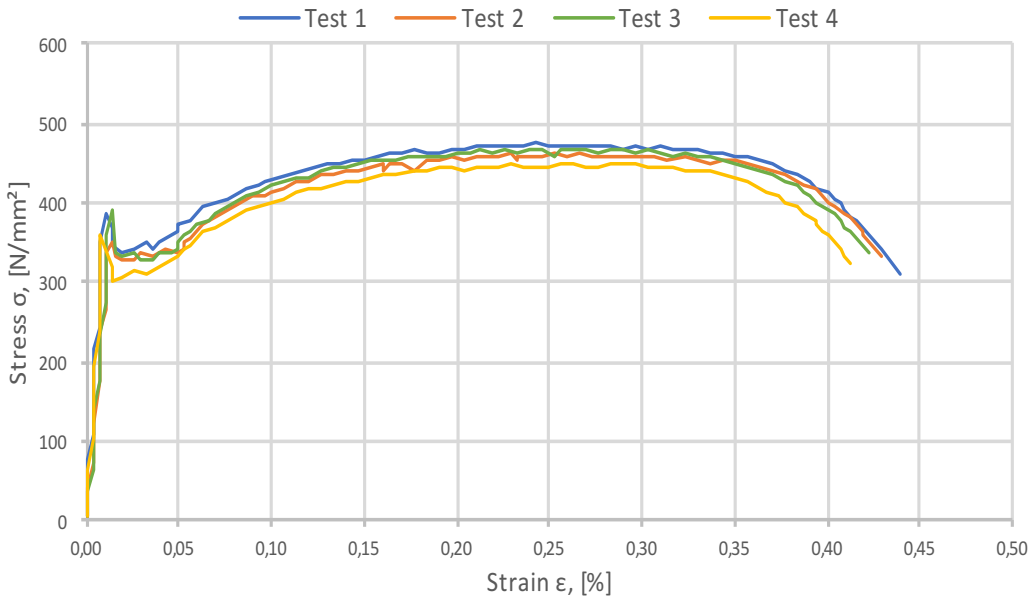


Stress-Strain diagram ($+25°C$)

| | Upper Yield Point | Lower Yield Point | Ultimate Strength | Fracture Point |
|---|---|---|---|---|
| **Test 1** | 384,306 | 337,408 | 474,211 | 309,963 |
| **Test 2** | 348,034 | 326,020 | 460,877 | 330,087 |
| **Test 3** | 389,894 | 330,441 | 466,112 | 338,116 |
| **Test 4** | 358,912 | 301,475 | 447,933 | 322,448 |
| **Average** | 370,287 | 323,836 | 462,283 | 325,154 |

Stress values ($+25°C$)

## A.2 Stress-Strain diagram ($-5°C$)

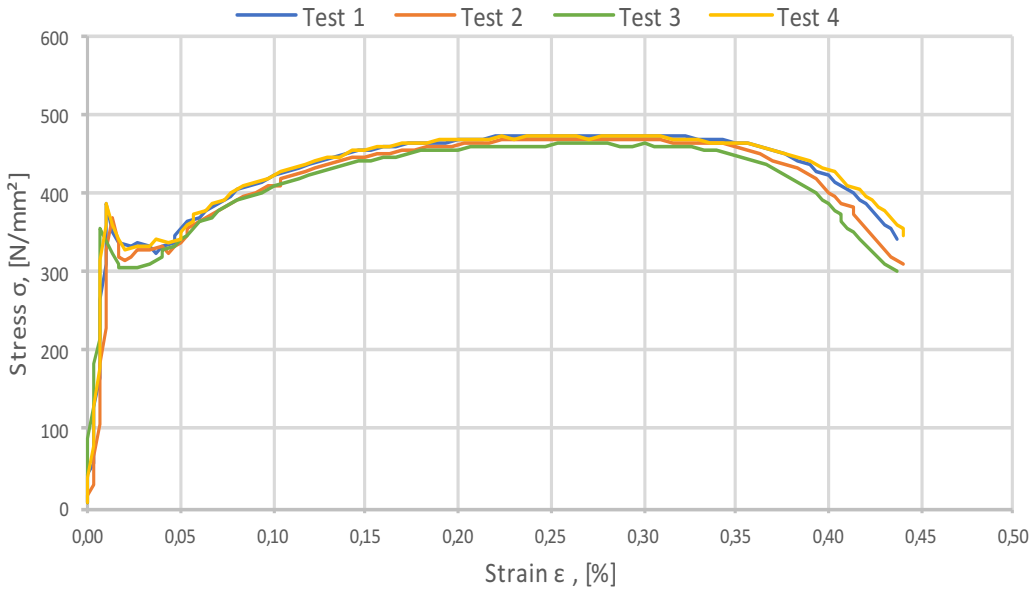


Stress-Strain diagram ($-5°C$)

| | Upper Yield Point | Lower Yield Point | Ultimate Strength | Fracture Point |
|---|---|---|---|---|
| **Test 1** | 386,534 | 325,498 | 475,340 | 341,546 |
| **Test 2** | 367,471 | 312,969 | 470,073 | 308,654 |
| **Test 3** | 354,703 | 305,825 | 463,495 | 301,120 |
| **Test 4** | 388,480 | 327,895 | 473,610 | 347,948 |
| **Average** | 374,297 | 318,047 | 470,629 | 324,817 |

Stress values ($-5°C$)

## A.3 Stress-Strain diagram ($-10°C$)

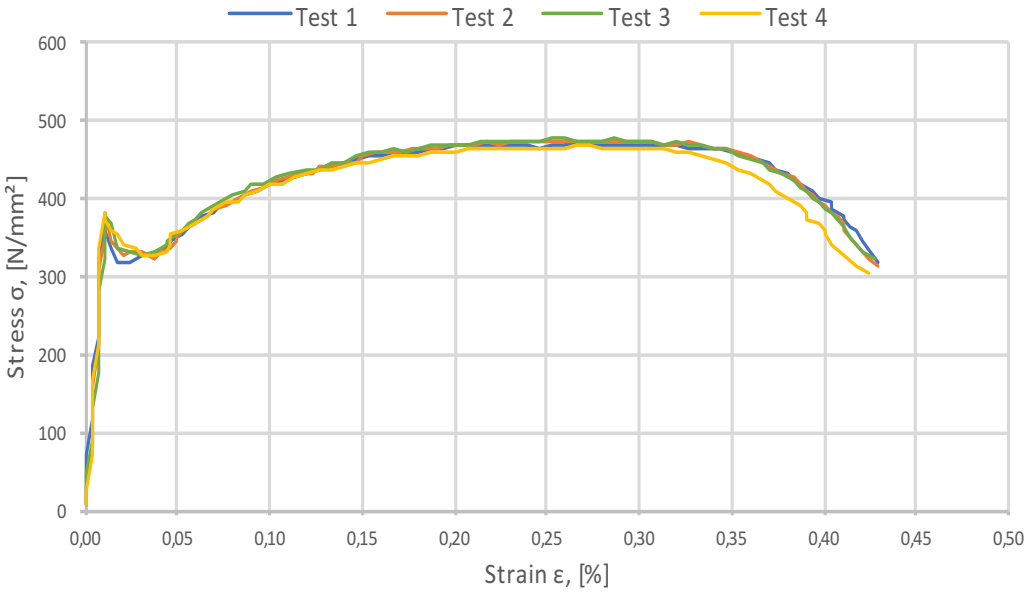


Stress-Strain diagram ($-10°C$)

| | Upper Yield Point | Lower Yield Point | Ultimate Strength | Fracture Point |
|---|---|---|---|---|
| **Test 1** | 365,278 | 317,709 | 470,993 | 315,516 |
| **Test 2** | 378,789 | 324,287 | 473,539 | 312,403 |
| **Test 3** | 375,747 | 326,48 | 475,555 | 319,442 |
| **Test 4** | 381,229 | 325,03 | 465,086 | 303,420 |
| **Average** | 375,26075 | 323,3765 | 471,29325 | 312,695 |

Stress values ($-10°C$)

## A.4 Stress-Strain diagram ($-15°C$)

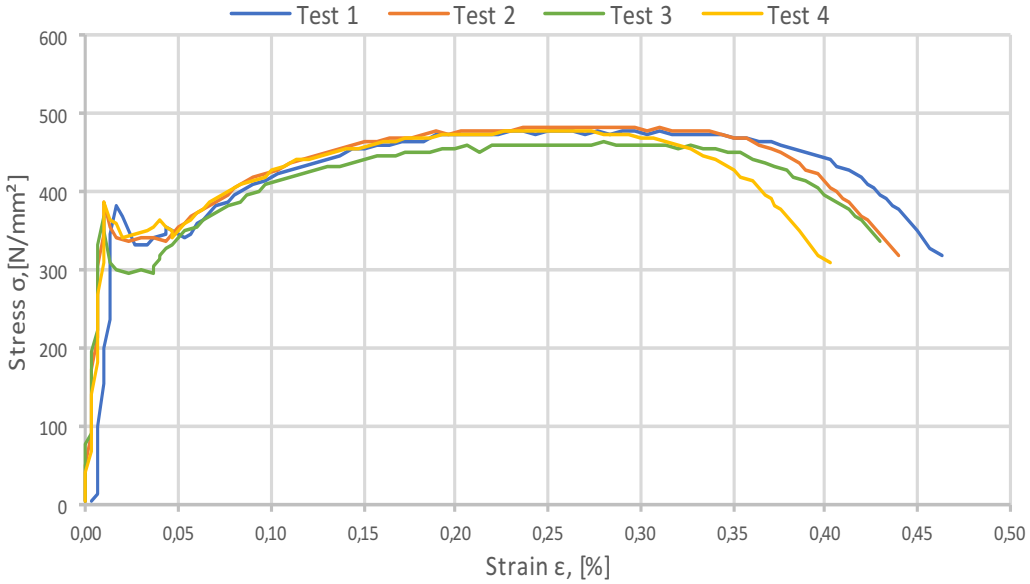


Stress-Strain diagram ($-15°C$)

| | Upper Yield Point | Lower Yield Point | Ultimate Strength | Fracture Point |
|---|---|---|---|---|
| **Test 1** | 381,335 | 334,190 | 479,693 | 318,275 |
| **Test 2** | 389,293 | 337,040 | 483,194 | 318,098 |
| **Test 3** | 369,982 | 296,064 | 463,388 | 338,116 |
| **Test 4** | 386,570 | 342,855 | 478,384 | 312,368 |
| **Average** | 381,795 | 327,537 | 476,165 | 321,714 |

Stress values ($-15°C$)

## A.5 Stress-Strain diagram ($-20°C$)

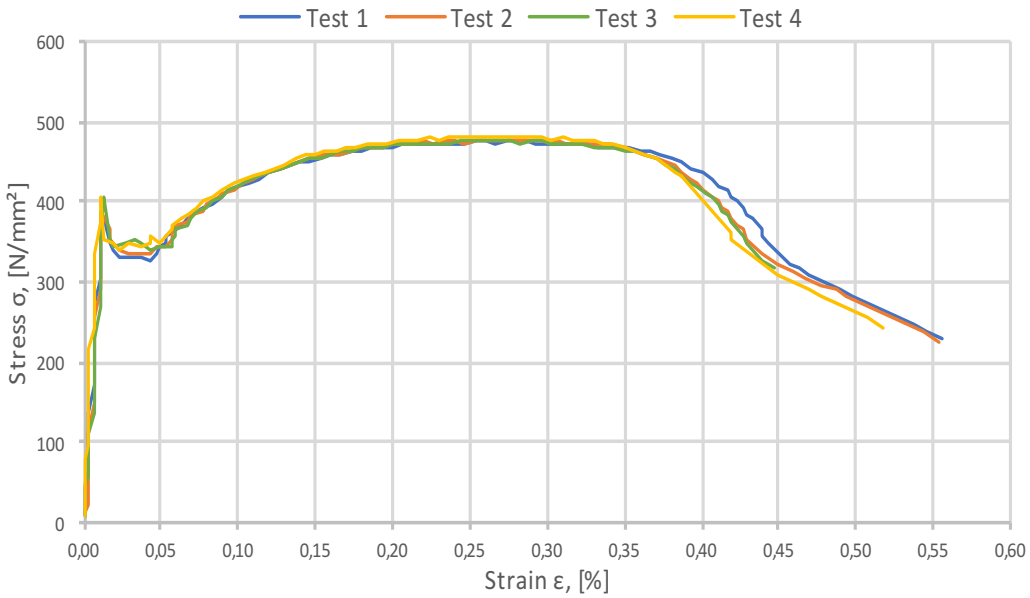


Stress-Strain diagram ($-20°C$)

| | Upper Yield Point | Lower Yield Point | Ultimate Strength | Fracture Point |
|---|---|---|---|---|
| **Test 1** | 387,383 | 327,506 | 474,918 | 229,714 |
| **Test 2** | 387,560 | 333,200 | 477,571 | 226,884 |
| **Test 3** | 405,810 | 339,460 | 475,590 | 316,718 |
| **Test 4** | 405,421 | 339,707 | 481,391 | 244,462 |
| **Average** | 396,544 | 334,968 | 477,368 | 254,445 |

Stress values ($-20°C$)

# B Thermography Results

## B.1 Profile plot ($+25°C$)

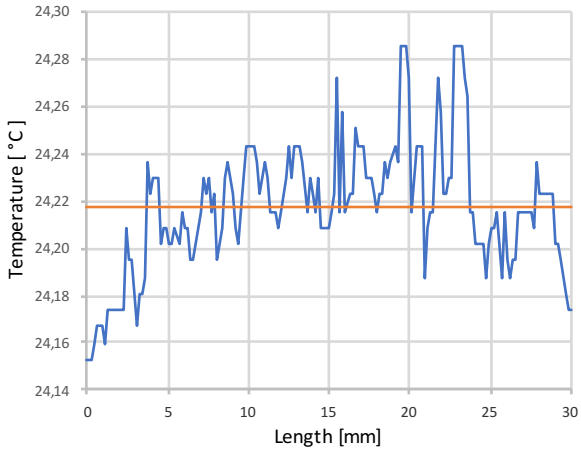


(a) Test1 Start

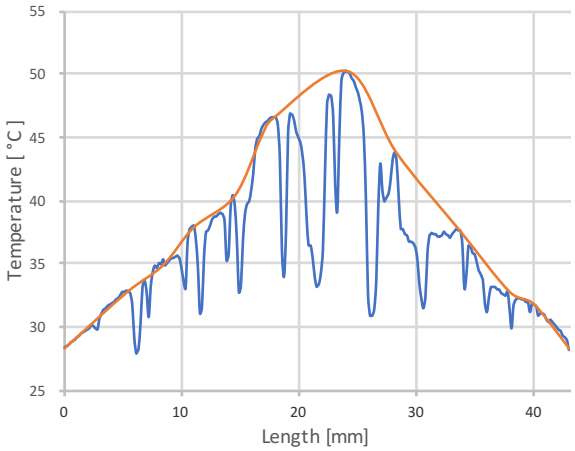


(b) Test1 End

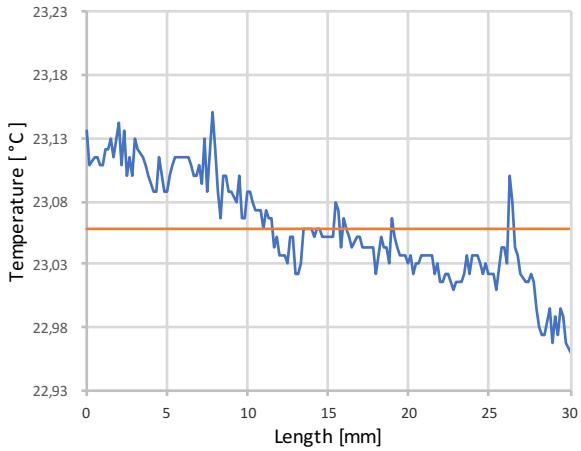


(c) Test2 Start

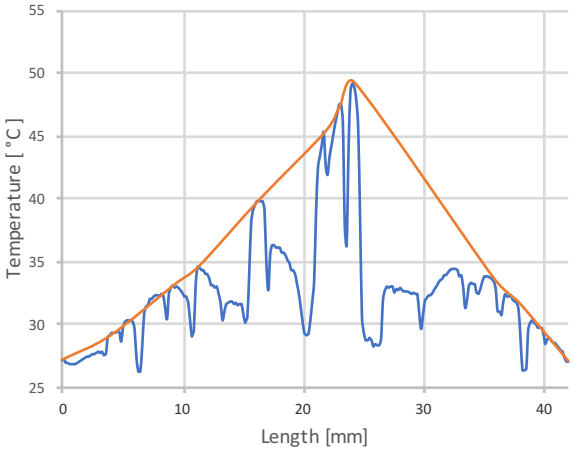


(d) Test2 End

IR results ($+25°C$)

## B.2 Profile plot ($-5°C$)

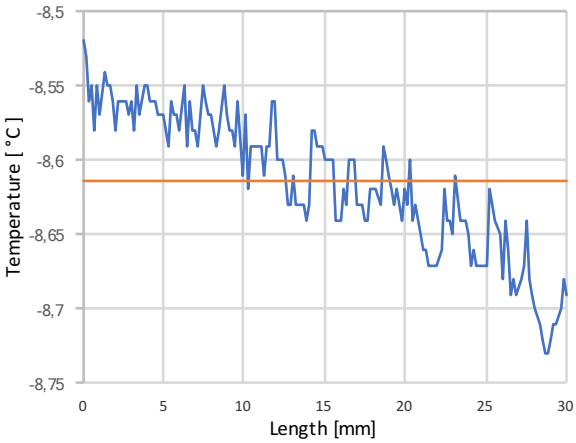


(a) Test1 Start

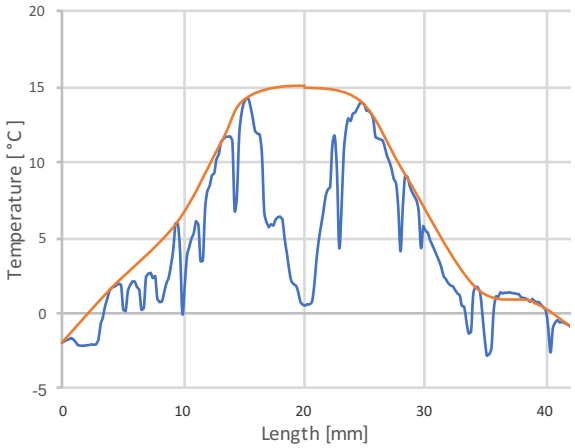


(b) Test1 End

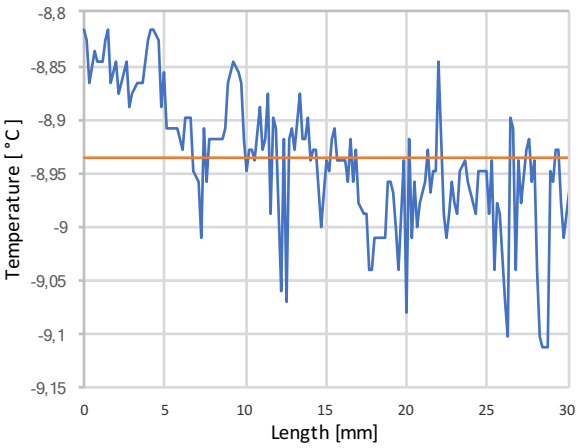


(c) Test2 Start

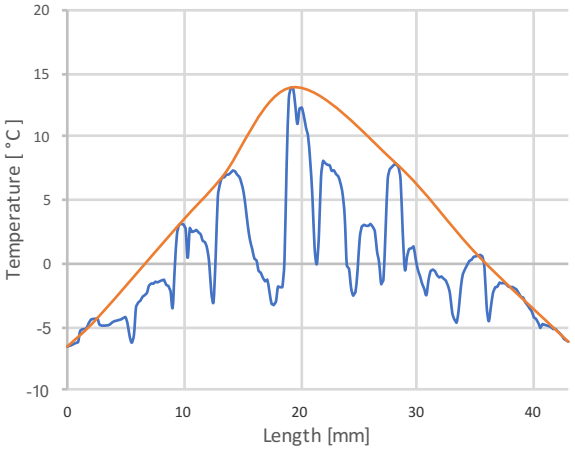


(d) Test2 End

IR results ($-5°C$)

## B.3 Profile plot ($-10°C$)

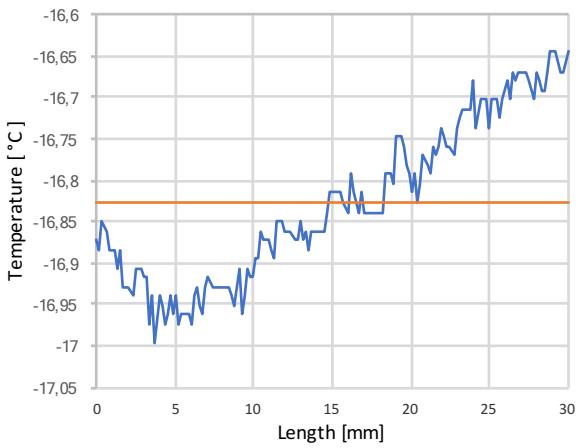


(a) Test1 Start

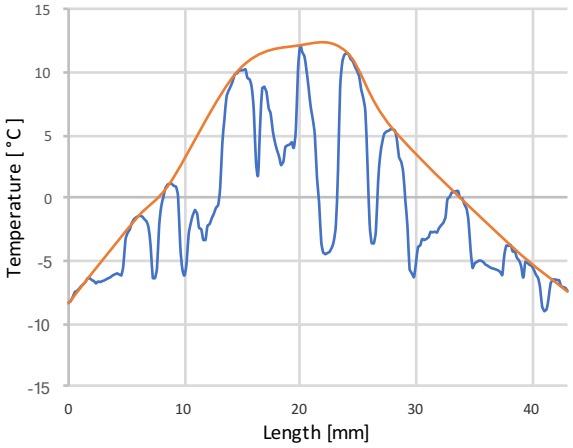


(b) Test1 End

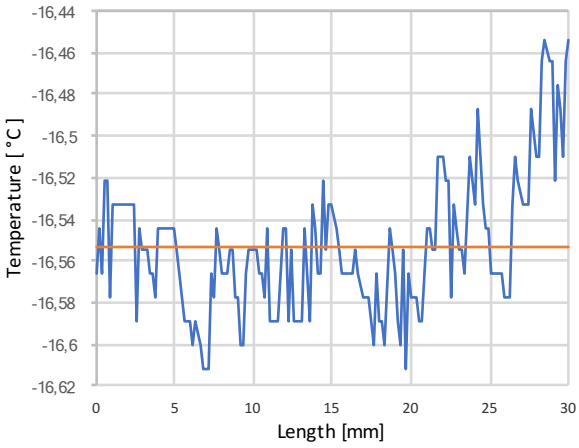


(c) Test2 Start

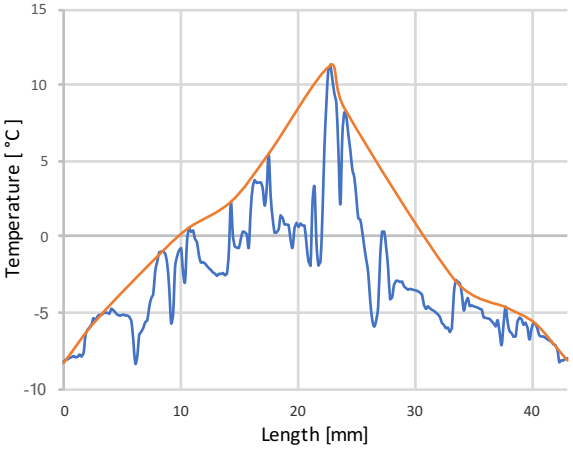


(d) Test2 End

IR results ($-10°C$)

## B.4 Profile plot ($-15°C$)

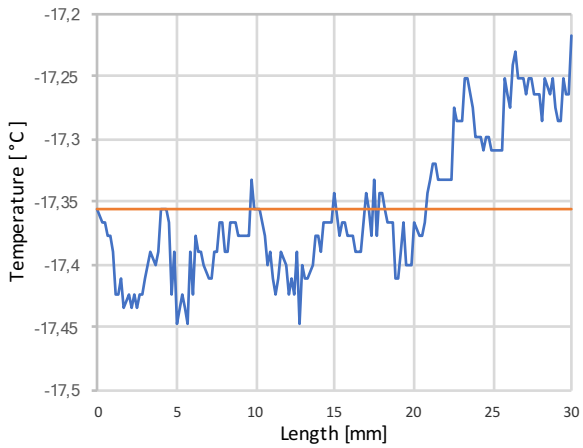


(a) Test1 Start

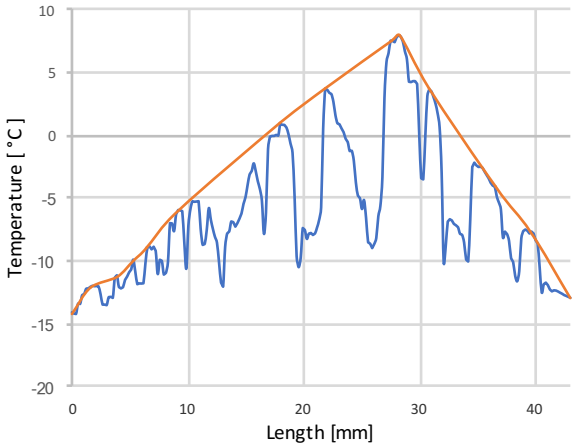


(b) Test1 End

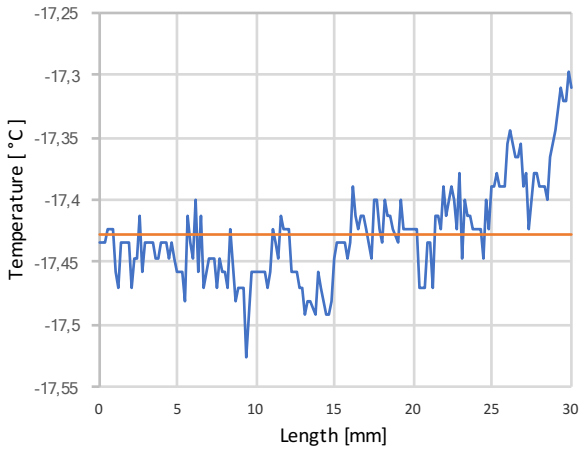


(c) Test2 Start

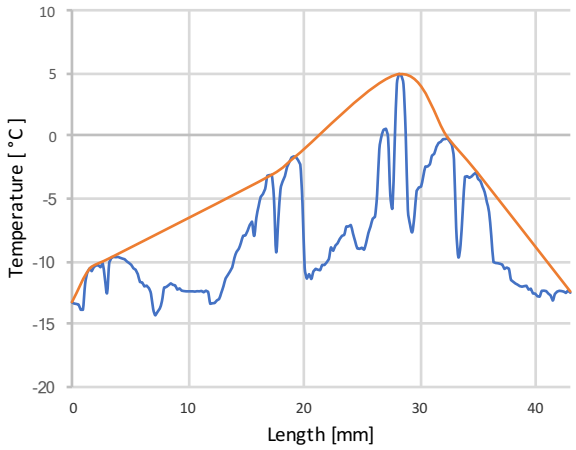


(d) Test2 End

IR results ($-15°C$)

## B.5 Profile plot ($-20°C$)

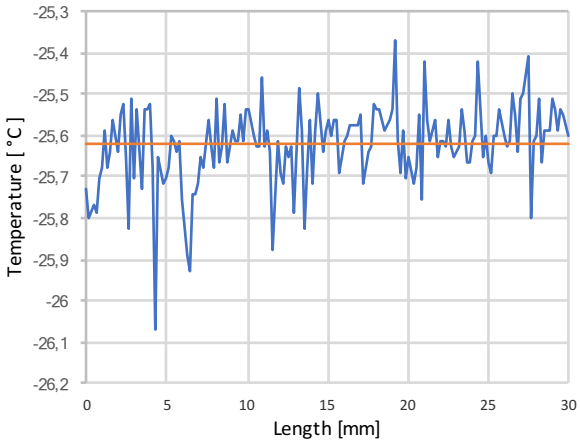


(a) Test1 Start

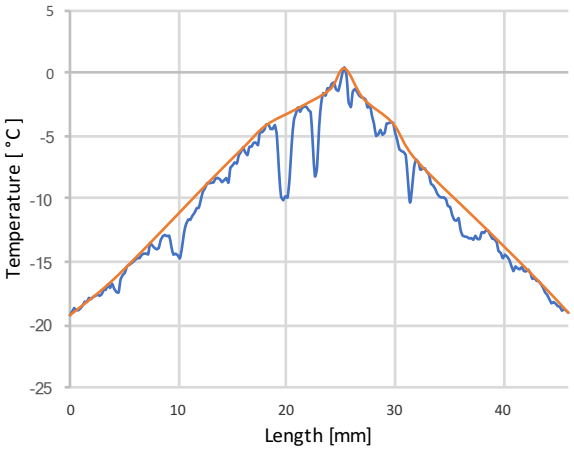


(b) Test1 End

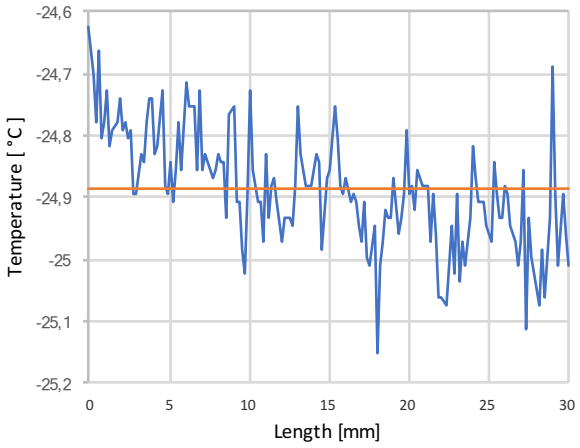


(c) Test2 Start

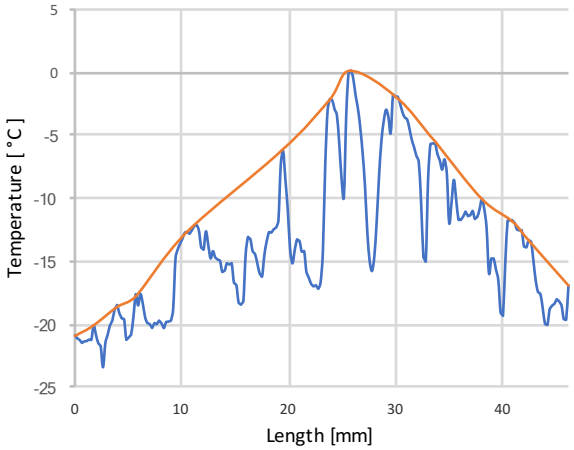


(d) Test2 End

IR results ($-20°C$)